



Evaluation of liquefaction potential by standard penetration test and shear wave velocity methods: a case study

Zeval Aytaş¹ · Nuray Alpaslan² · Ferhat Özçep³

Received: 24 May 2022 / Accepted: 5 July 2023 / Published online: 21 July 2023
© The Author(s), under exclusive licence to Springer Nature B.V. 2023

Abstract

Dynamic loads such as earthquakes can cause major failure to soil, and the foremost of these failure is soil liquefaction. In engineering studies, liquefaction analyses can be performed by different methods based on the results of field and laboratory experiments. In this study, the liquefaction potential of the soils of the Batman settlement zone, located close to the East Anatolian Fault Zone in Türkiye, was evaluated. In the study area, Meydan site consists of low-medium plasticity clay (CL) at a depth of 1.5–3 m and silty sand (SM) at a depth of 3.5–12.45 m; Bahçelievler site consists of low-medium plasticity clay (CL) at a depth of 1.5–7 m and silty sand (SM) at a depth of 7–15 m. For liquefaction analysis, magnitudes and accelerations of design earthquake were selected as 0.30 g for accelerations, and 7.5 and 6.5 for magnitudes. For this purpose, the effects of soil and earthquake parameters on soil liquefaction were evaluated using the standard penetration test (SPT) and shear wave velocity (V_s) methods with the Microsoft Excel-based SoilEngineering program and the obtained results were correlated and discussed. It is emphasized in this work that liquefaction potential analyses using soil and earthquake parameters provide more reliable results. In addition, the soil strata of locations where the liquefaction risk potential is high were found to have total settlement of approximately 36.87 to 36.2 cm, parallel to the high liquefaction risk, and it was determined that there may be high settlement in the area.

Keywords Shear wave velocity (V_s) · Liquefaction analysis · SoilEngineering · Standard penetration test (SPT) · Settlement

✉ Nuray Alpaslan
nuray.alpaslan@batman.edu.tr

Zeval Aytaş
z.aytas_21@hotmail.com

Ferhat Özçep
ferozcep@iuc.edu.tr

¹ Acacia Mining Operations Firm, 37452 Küreçayı, Kastamonu, Turkey

² Department of Civil Engineering, Faculty of Engineering and Architecture, Batman University, 72100 Batman, Turkey

³ Department of Geophysics Engineering, Cerrahpaşa Faculty of Engineering and Architecture, İstanbul University, 34320 İstanbul, Turkey

Abbreviations

γ	Unit volume weight
σ_v	Overburden pressure
σ'_v	Effective overburden pressure
a_{\max}	Design earthquake acceleration
C_B	Borehole correction factor
C_E	Hammer energy ratio
C_R	Rod length correction factor
C_S	Correction factor for samples
C_V	Factor to correct measured shear wave velocity results
C_N	Factor to correct measured standard penetration test results
CRR	Cyclic resistance ratio
CRR _{7.5}	Cyclic resistance ratio for $M_w = 7.5$
CSR	Cyclic stress ratio
FC	Fine grain content
M_w	Moment magnitude
MSF	Magnitude scaling factor
$(N_1)_{60}$	Corrected standard penetration value
r_d	Stress reduction factor
SF	Safety factor
SPT	Standard penetration test
V_s	Measured shear wave velocity
V_{s1}	Corrected shear wave velocity
Vsc1	Corrected shear wave velocity
z	Depth

1 Introduction

Earthquakes, which can be defined as dynamic loads that disrupt the equilibrium of the soil, cause cyclic loading. The behavior of soil against these cyclic stresses varies depending on soil type, physical properties, earthquake characteristics, dynamic behavior, and stress-displacement properties. Therefore, cyclic loads cause deformations of different sizes in each soil type (Koc 2007). And then soil failure may lead to damage because of liquefaction. Liquefaction is the process in which soil changes from a solid phase to a liquid phase, often as a result of cyclic loads during earthquakes that decrease effective stress and increase pore water pressure in water-saturated soil strata.

The term “liquefaction” was coined by Mogami and Kubo in 1953 (Kramer 1996), and the devastating effects of liquefaction on soil and local structures during earthquakes, such as the Alaska ($M_w = 9.2$) and Niigata ($M_w = 7.5$) earthquakes in 1964, have drawn significant attention to this phenomenon.

As a result, extensive field and laboratory experiments have been conducted to investigate the physics and mechanisms of liquefaction. The first major studies in this field include “Liquefaction of Saturated Sands During Cyclic Loading” by Seed and Lee (1966), “An Experimental Study of Liquefaction of Saturated Sands” by Yoshimi (1967), and “Characteristics of Liquefied Sands During Mino-Owari, Tohankai, and Fukui Earthquakes” by Kishida (1969).

Several researchers, including Castro (1969), Seed and Idriss (1971), Seed (1976) and Stokoe et al. (1988), have conducted studies based on field measurement data obtained from the standard penetration test (SPT), cone penetration test (CPT), and shear wave velocity (V_s) methods for laboratory studies and liquefaction analysis. After the 1964 Niigata and Alaska earthquakes, Seed and Idriss developed a method for calculating soil liquefaction potential, which they called the “simplified method,” in 1971. Their method was subsequently improved upon by Seed et al. (1975a, b, 1983, 1985) and Youd and Idriss (2001). In the early 2000s, further studies were conducted to refine this approach, including work by Youd et al. (2001), Cetin et al. (2004b), Idriss and Boulanger (2008), and Boulanger and Idriss (2014). These studies have contributed to significant improvements in the calculation of soil liquefaction potential.

Using SPT-N values and V_s data, which are two significant parameters in determining the risk of liquefaction, many researchers have developed various empirical formulas to be applied (Dikmen, 2009; Akın et al. 2011). In addition, many researchers have performed liquefaction analysis using SPT-N values and V_s data (Ulamis and Kilic 2008; Karakas and Coruk 2010; Ulamis and Kilic 2012; Akkaya et al. 2018a; Tunusluoğlu and Karaca, 2018; Eyisüren et al. 2023). Researchers have performed several studies to determine liquefaction potential using V_s , which is a significant parameter in evaluations of the dynamic properties of soils (Dobry et al. 1981; Tokimatsu and Yoshimi 1983; Andrus and Stokoe 2000; Uyanık 2002; Özçep et al. 2003; Zarif et al. 2004; Zarif et al. 2005; Özçep and Zarif 2006; Uyanık, 2006; Dadashpour et al. 2009; Özçep and Zarif 2009; Uyanık and Taktak 2009; Kayen et al. 2013; Uyanık et al. 2013a; Özçep et al. 2014; Porcino and Tomasello 2019; Uyanık 2020; Duan et al. 2023).

In this study, liquefaction analyses were performed using the Microsoft Excel-based SoilEngineering program (Özçep, 2010) with SPT and V_s field data obtained in Batman Province, which is located close to the East Anatolian Fault Zone in Türkiye. Batman Province, located in the Southeastern Anatolia Region of Türkiye, has various soil problems and is also experiencing rapid construction development. Thus, the effects of earthquake parameters and soil properties are compared and discussed in this study based on liquefaction analyses conducted for Batman Province. In addition, the importance of evaluating soil properties and earthquake parameters together in liquefaction potential analyses is emphasized.

2 Materials and methods

The first simplified studies on evaluating the liquefaction potential of soil through stress were conducted by Seed and Idriss (1971). In their work, the safety of the soil in the face of liquefaction during an earthquake was calculated by comparing the cyclic resistance ratio (CRR) of the soil to the cyclic stress ratio (CSR) resulting from the earthquake. The CSR during an earthquake as described by Seed and Idriss (1971) is shown in Equ. 1.

$$CSR = 0.65 * (a_{\max}/g) \left(\frac{\sigma_0}{\sigma'_0} \right) * r_d \quad (1)$$

In Equ. 1, g represents gravitational acceleration; σ_0 and σ'_0 signify the overburden pressure and effective overburden pressure at the depth (z) at which the liquefaction analysis

was conducted, respectively; and r_d is the stress reduction factor, which is determined by the depth-based expressions given in Equ. 2 and 3 (Liao and Whitman 1986).

$$r_d = 1.0 - 0.00765 * z \quad z \leq 9.15\text{m} \tag{2}$$

$$r_d = 1.174 - 0.0267 * z \quad 9.15\text{m} < z \leq 23 \text{ m} \tag{3}$$

2.1 Liquefaction analysis according to the Turkish Building Earthquake Code (TBEC 2018)

The Turkish Building Earthquake Code (TBEC, 2018) aimed to gather earthquake data for four different levels of earthquake ground motion and earthquake parameters based on the “Earthquake Hazard Map of Türkiye” (EHMT) (<https://tdth.afad.gov.tr/>). In accordance with the TBEC, the peak ground acceleration (PGA), which represents the largest horizontal ground acceleration value, was determined for the site based on the seismic hazard map values at the location coordinates. This map can be accessed through the website of the Disaster and Emergency Management Presidency (AFAD). To this end, four earthquake hazard maps were prepared for four different levels of earthquake ground motion, including two dimensionless spectral acceleration maps and two maps containing spectral acceleration coefficients for short period map spectral acceleration (S_S) and spectral acceleration coefficients for a period of 1.0 s (S_1). The map spectral acceleration coefficients were converted to design spectral response acceleration (S_{DS} and S_{D1}) by employing local effect coefficients chosen based on the local soil class, and horizontal elastic design spectra were derived from these coefficients (Fig. 1).

The determined map spectral acceleration coefficients S_S and S_1 were converted to design spectral response accelerations S_{DS} and S_{D1} as shown in Equ. 4 and Equ. 5 (TBEC, 2018).

$$S_{DS} = S_S \cdot F_s \tag{4}$$

$$S_{D1} = S_1 \cdot F_1 \tag{5}$$

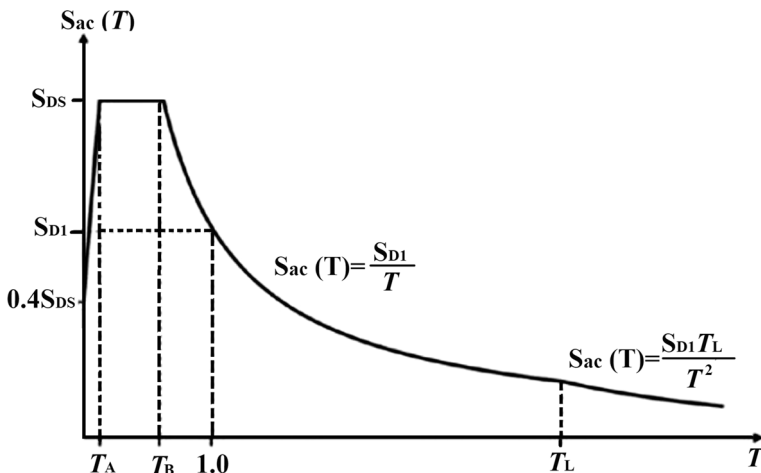


Fig. 1 Horizontal elastic design spectrum (TBEC 2018)

Table 1 Local soil impact coefficient (F_s) for the short period zone (TBEC 2018)

Local soil class	Local soil impact coefficient (F_s) for the short period region					
	$S_S \ll 0.25$	$S_S = 0.50$	$S_S = 0.75$	$S_S = 1.00$	$S_S = 1.25$	$S_S \gg 1.50$
ZA	0.8	0.8	0.8	0.8	0.8	0.8
ZB	0.9	0.9	0.9	0.9	0.9	0.9
ZC	1.3	1.3	1.2	1.2	1.2	1.2
ZD	1.6	1.4	1.2	1.1	1.0	1.0
ZE	2.4	1.7	1.3	1.1	0.9	0.8
ZF	Site-specific soil behavior analysis					

Table 2 Local soil impact coefficient (F_1) for the short period zone (TBEC 2018)

Local soil class	Local soil impact coefficient (F_1) for a period of 1.0 s					
	$S_S \ll 0.10$	$S_S = 0.20$	$S_S = 0.30$	$S_S = 0.40$	$S_S = 0.50$	$S_S \gg 0.60$
ZA	0.8	0.8	0.8	0.8	0.8	0.8
ZB	0.8	0.8	0.8	0.8	0.8	0.8
ZC	1.5	1.5	1.5	1.5	1.5	1.4
ZD	2.4	2.2	2.0	1.9	1.8	1.7
ZE	4.2	3.3	2.8	2.4	2.2	2.0
ZF	Site-specific soil behavior analysis					

In Equ. 4, S_S represents the short period spectral acceleration value and F_S is the local ground effect coefficient for the short period region. S_{DS} is the short period (0.2 s) dimensionless design spectral response acceleration. In S_{DS} , “S” stands for spectral acceleration, the subscript “D” stands for design, and the subscript “S” stands for short. Local ground effect coefficients F_S and F_1 are given in Tables 1 and 2.

Horizontal design spectrum corner periods were defined based on T_A and T_B with S_{DS} and S_{D1} , as given in Equ. 6 and Equ. 7. The transition period to the constant displacement region was accepted as $T_L = 6$ s (TBEC, 2018).

$$T_A = 0.2 \frac{S_{D1}}{S_{DS}} \tag{6}$$

$$T_B = \frac{S_{D1}}{S_{DS}} \tag{7}$$

Within the framework of the Turkish Building Earthquake Code (TBEC, 2018), it was determined during SPT analyses performed in the boring stage that some physical factors had effects on the test and corrections for those factors were proposed to ensure that the test results could be evaluated in line with a common standard. The blow counts measured for a field during SPT-N analysis depend on many factors including overburden pressure, borehole diameter, rod length, energy ratio, and type of sampler. For this reason, the SPT-N values to be

used in calculations based on SPT should be corrected first (Table 3). In the present study, the corrected SPT-N values for an overburden pressure of 100 kPa and energy efficiency of 60%, $N_{1,60}$, were obtained from Equ. 8.

$$N_{1,60} = N_{60} * C_N \Rightarrow N_{60} = N_* C_R * C_S * C_B * C_E \tag{8}$$

The left-hand side of Equ. 8 represents the corrected SPT blow count, N is the measured number of SPT blow counts in a given field, C_N is the depth correction factor, C_E corresponds to the hammer energy ratio (ER) correction factor, C_B is the borehole diameter correction factor, C_R denotes the rod length correction factor, and C_S is a correction factor for samplers with or without liners.

The curve separating the regions where liquefaction occurs and where it is not observed in cases of earthquakes of magnitude $M_w=7.5$ for clean sands with less than 5% fine grains ($FC \leq 5\%$) was defined as the clean sand curve by Youd et al. (2001) (Fig. 2). The cyclic resistance ratio ($CRR_{7.5}$) for this condition can be formulated as shown in Equ. 9.

$$CRR_{7.5} = \frac{1}{34 - N_{1,60f}} + \frac{N_{1,60f}}{135} + \frac{50}{[10N_{1,60f} + 45]^2} - \frac{1}{200} \tag{9}$$

The Turkish Building Earthquake Code (TBEC, 2018) also addresses the determination of liquefaction potential according to shear wave velocity (V_s), which is one of the dynamic properties of soils. V_s values can be measured using classical geophysical methods such as seismic refraction and seismic reflection, as well as borehole geophysical methods such as cross-hole, down-hole, and seismic CPT or analysis methods such as multichannel analysis of surface waves (MASW) and spectral analysis of surface waves (SASW).

Liquefaction resistance depending on V_s as obtained by seismic experiments was calculated based on the formula of Andrus and Stokoe (2000) as shown in Equ. 10.

Table 3 SPT correction factors (TBCE 2018)

Correction factor	Equipment variable	Correction variable
Overburden pressure (C_N)	–	$(95.76/\sigma'_v) \ll 1.7$
Energy ratio (C_E)	Donut hammer	0.45–1.00
	Safety hammer	0.60–1.17
	Automatic impact hammer	0.90–1.60
Drill diameter (C_B)	65–115 mm	1.0
	150 mm	1.05
	200 mm	1.15
Rod length (C_R)	3–4 m	0.75
	4–6 m	0.85
	6–10 m	0.95
	10–30 m	1.0
Sampler type (C_S)	Standard sampler without an inner tube	1.0
		1.1–1.3

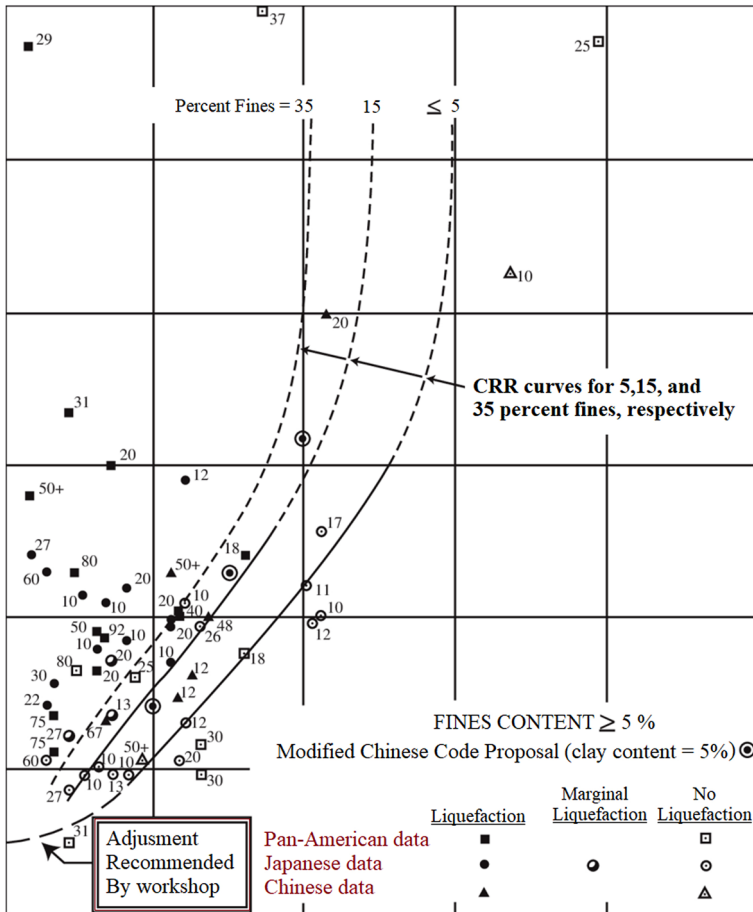


Fig. 2 Corrected SPT (N)-CSR chart in clean and silty sand for an earthquake with a magnitude of 7.5 (Youd et al. 2001)

$$CRR_{7.5} = 0.022 \left[\frac{(V_{s1})}{100} \right]^2 + 2.8 \left[\frac{1}{215 - (V_{s1})} - \frac{1}{215} \right] \tag{10}$$

In this method, the S-wave velocity (V_{s1}) must first be corrected in order to be used in liquefaction calculations (Fig. 3). Here, corrected S-wave velocity (V_{s1}) was calculated using the overburden load and V_s relative to vertical stress as shown in Equ. 11.

$$V_{s1} = V_s (P_a / \sigma'_0)^{0.25} \tag{11}$$

In the equation above, P_a is atmospheric pressure of 100 kPa and σ'_v is the effective vertical stress measured in kPa. V_{s1}^* is the upper limit of shear wave velocity at which liquefaction occurs depending on the fine grain ratio (FC). In the equation for sandy soil, V_{s1} is as follows:

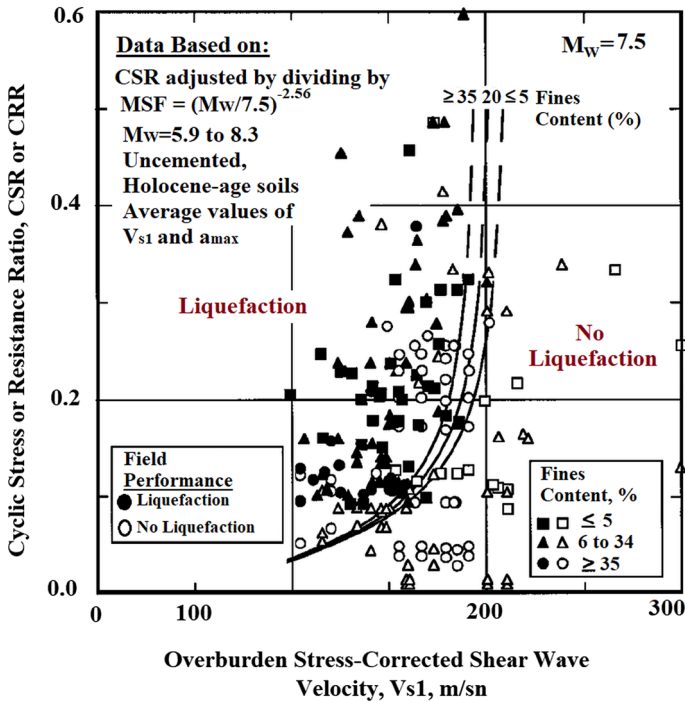


Fig. 3 Corrected V_s -CSR Chart for clean and silty sands for an earthquake with a magnitude of 7.5 (Andrus and Stokoe 2000)

$$CRR_{7.5} = 0.022 \left[\frac{(V_{s1})^2}{100} \right] + 2.8 \left[\frac{1}{215 - 0.5(FC - 5) - (V_{s1})} - \frac{1}{215 - 0.5(FC - 5)} \right]$$

$5\% < F.C. < 35\%$

(12)

$$CRR_{7.5} = 0.022 \left[\frac{(V_{s1})^2}{100} \right] + 2.8 \left[\frac{1}{200 - (V_{s1})} - \frac{1}{200} \right] \quad F.C. \gg 35\%$$

(13)

2.2 Liquefaction safety conditions

The liquefaction potential of a soil profile is assessed by comparing its loading and resistance. The safety factor is determined by considering the cyclic resistance ratio (CRR) of the soil against liquefaction and the cyclic stress ratio (CSR) induced by the earthquake. Equation 2.19 presents the safety factor calculated using the corrected SPT-(N1)60 values proposed by Youd et al. (2001) and Idriss and Boulanger (2008). Moreover, Equ. 14 incorporates the effect of the magnitude scaling factor (MSF) on the safety factor against liquefaction.

$$FS = \frac{CRR}{CSR}MSF \tag{14}$$

As a general rule, no liquefaction is expected for safety factors greater than 1.2, potential liquefaction is expected for safety factors between 1 and 1.2, and liquefaction is expected for safety factors less than 1 (Seed and Idriss, 1971). To consider the impact of duration effects (number of loading cycles) on the initiation of liquefaction, the magnitude scaling factor (MSF) is employed. Figure 4 illustrates the relationships between the MSF factors (Idriss and Boulanger 2010), which are determined using Equ. 15. Idriss (1999) developed this earthquake magnitude correction factor.

$$MSF = 6.9\exp\left(\frac{-M_w}{4}\right) - 0.06 \quad M_w > 5.2 \tag{15}$$

According to the Turkish Building Earthquake Code (2018), the safety factor against liquefaction is to be calculated with Equ. 16. If the condition given in Equ. 16 is not met, then liquefaction is to be expected, and if the condition is met, then liquefaction is not expected.

$$FS_L = \frac{\tau_R}{\tau_{earthquake}} \gg 1.10 \tag{16}$$

In Equ. 16, τ_R and $\tau_{earthquake}$ refer to liquefaction resistance and the average cyclic shear stress caused by the earthquake on the soil, respectively.

2.3 Soil settlement due to liquefaction

The generation of excessive pore water pressure during an earthquake can result in cyclic soil movements during and after the event. The dissipation of pore water pressure following

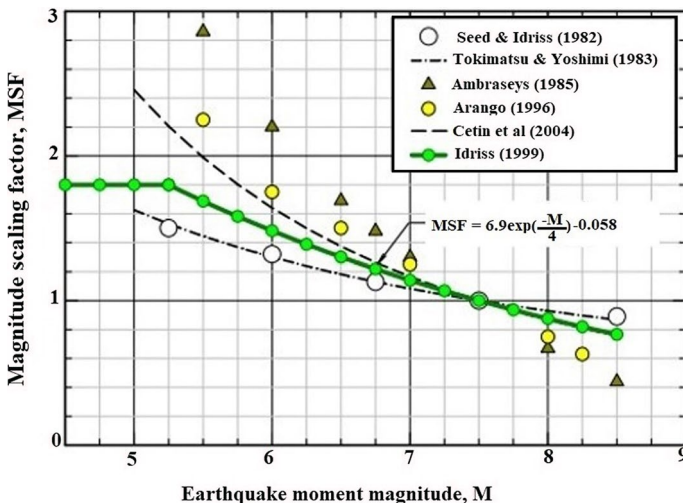


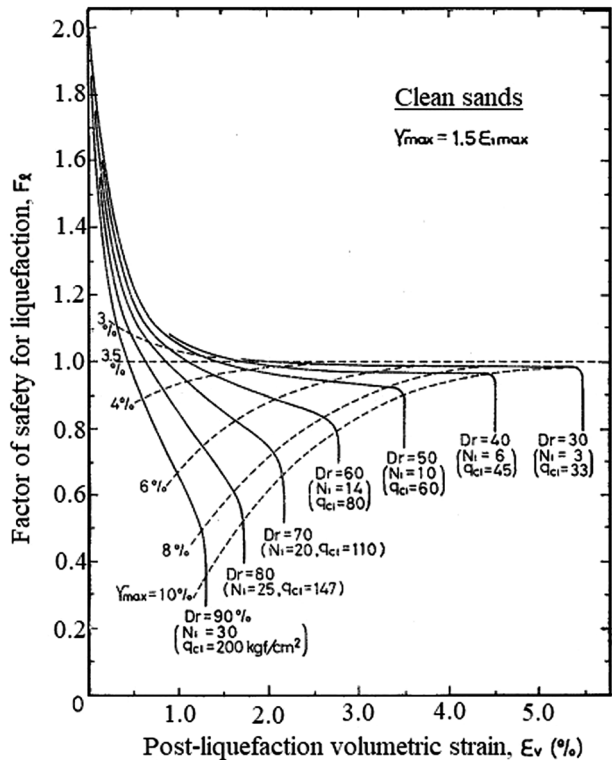
Fig. 4 Magnitude scaling factor (MSF) relationships (Idriss and Boulanger 2010)

the earthquake leads to soil volume changes. Such volumetric strains, which cause soil settlement due to liquefaction, can impact the performance of structures and cause strains on their bases. Empirical studies by Lee and Albaisa (1974) and Yoshmini (1975) investigated the volumetric changes caused by excessive pore water pressure dispersion in saturated sands under cyclic loads in laboratory conditions. More recent related studies proposed empirical maps for estimating volumetric strain in liquefied clean sands. These include Tokimatsu and Seed (1987), Ishihara and Yoshimine (1992), Shamoto (1998), Pradel (1998), Unutmaz and Çetin (2005), and Bilge and Çetin (2006). These maps were developed based on dynamic triaxial compression tests on sands of varying relative densities. Ishihara and Yoshimine (1992) developed a method that evaluates the volumetric strain of each layer separately in calculations for soil settlement after an earthquake. The calculation for soil settlement after an earthquake is given in Equ. 17. The volumetric strain can be determined using the graph in Fig. 5, which depends on the safety factor (SF) and the relative density in soil layers (Dr).

$$S_{sat} = (\epsilon_V/100) * z \tag{17}$$

In Equ. 17, z is the thickness of the layer in meters, ϵ_V is the volumetric strain, and S_{sat} is the corresponding saturated soil layer.

Fig. 5 The relationships between safety factor, F_s , and post-liquefaction volumetric strain ϵ_V (Ishihara and Yoshimine 1992)



2.4 SoilEngineering: a Microsoft Excel® spreadsheet program

In recent years, many programs that provide computer-aided solutions to analyze liquefaction potential through the use of different parameters have been developed in the field of geotechnical engineering. Some of these programs include LIQUITER, which works based on the method of Seed and Idriss (1971) and enables calculations of safety factors against liquefaction for saturated cohesionless soils subjected to earthquake loads; LiqIT, which enables liquefaction analysis of saturated loose soils; SPTLIQ, which enables calculations of liquefaction potential and settlement caused by earthquakes; LiquefyPro, which enables evaluations of liquefaction potential and earthquakes; and CUMLIQ, which enables calculations of the liquefaction potential of alluvial soils (Tolon, 2013). In addition, soiLique, developed by Bekin and Özçep (2021), offers the first deterministic soil liquefaction analysis method based on MATLAB that includes a graphical user interface (GUI). The fundamental characteristic of soiLique is its independence from MATLAB®. In other words, soiLique can be used without MATLAB® by installing MATLAB® Runtime Environment v9.7 to run. In the present study, liquefaction analysis calculations were performed using the SoilEngineering program developed by Özçep (2010). It is an open coded software. SoilEngineering is a free Microsoft Excel-based program that is widely used for the geotechnical and geophysical analysis of soils, especially in Türkiye. Its application in geotechnical and geophysical analysis of soils under static and dynamic loads is very practical. Analysis of soil problems in geotechnical research can be easily performed using this program. In addition, this program also has the advantage of calculating data numerically and presenting the results with visual graphs (Figs. 6, 7).

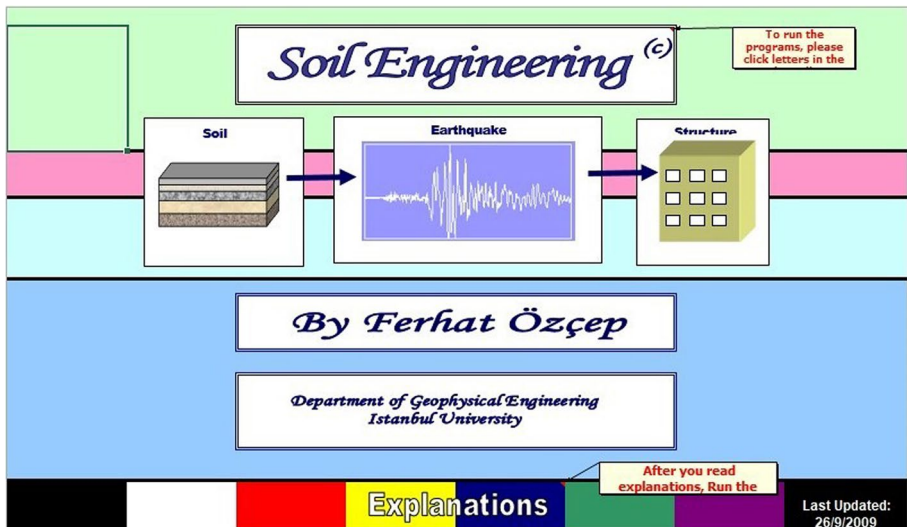


Fig. 6 SoilEngineering Microsoft Excels Program overview

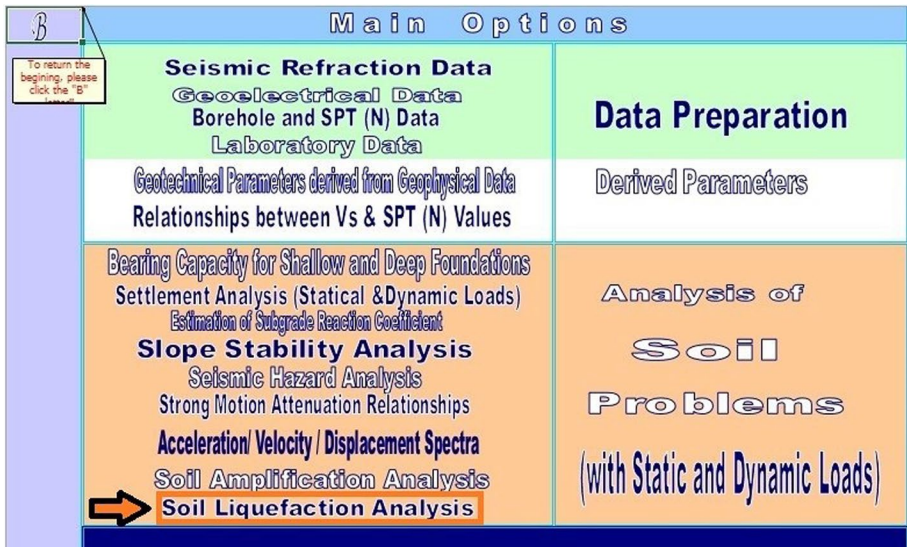


Fig. 7 SoilEngineering Microsoft Excels Program Main Options view

3 Geological setting

Batman Province is located in the Southeastern Anatolia Region of Türkiye. The approximate area of the province is 4,477 km² and it is located at an altitude of 550 m. The oldest stratigraphic unit observed in and around Batman Province is the Hoya Formation of the Midyat Group, which consists of a Lower Eocene-Lower Oligocene sparse argillaceous limestone level with limestone, dolomitic limestone, and dolomites. This formation is concordant with the Gercüş Formation near Hasankeyf, located in the vicinity of Batman Province (Tuna 1973; Açıkbaş and Baştuğ 1975; Perinçek 1979). The Hoya Formation is composed of massive and medium to thickly layered, sometimes thinly to medium layered, cream, beige, gray, light gray, black, or white nummulite, miliolid, algal, echinoid, gastropod, lamellar, shell-sediment, hard limestones with sporadic dolomitic limestones. This stratigraphic unit, consisting of white, red, coffee-colored, green, beige, and gray gypsum, anhydride, shale, dolomite, and sandy alluvion dolomites, was first identified by Bolgi (1961). The Germik Formation, consisting of Oligocene-aged argillaceous limestones and sporadic dolomitic limestone, overlies the Hoya Formation. While the Germik Formation concordantly overlies the Hoya Formation, it is nonconcordantly overlain by the Şelmo Formation. The Germik Formation consists of white, beige, gray, and dirty yellow soft gypsum, anhydride, shale, and dolomites that are not resistant to dispersive physical conditions. The Germik Formation's thickness is no more than 465 m (Eren et al. 2012). These formations are nonconcordantly overlain by the Şelmo Formation, which is composed of Middle-Upper Miocene conglomerate, sandstone, and mudstone. The Şelmo Formation constitutes a large part of the study area located in the city center of Batman (Eren et al. 2012). The Quaternary-aged basalts forming Kira Mountain overlie the Şelmo Formation, and Quaternary units consisting of alluviums surface around the Batman Creek Valley and Batman (Fig. 8).

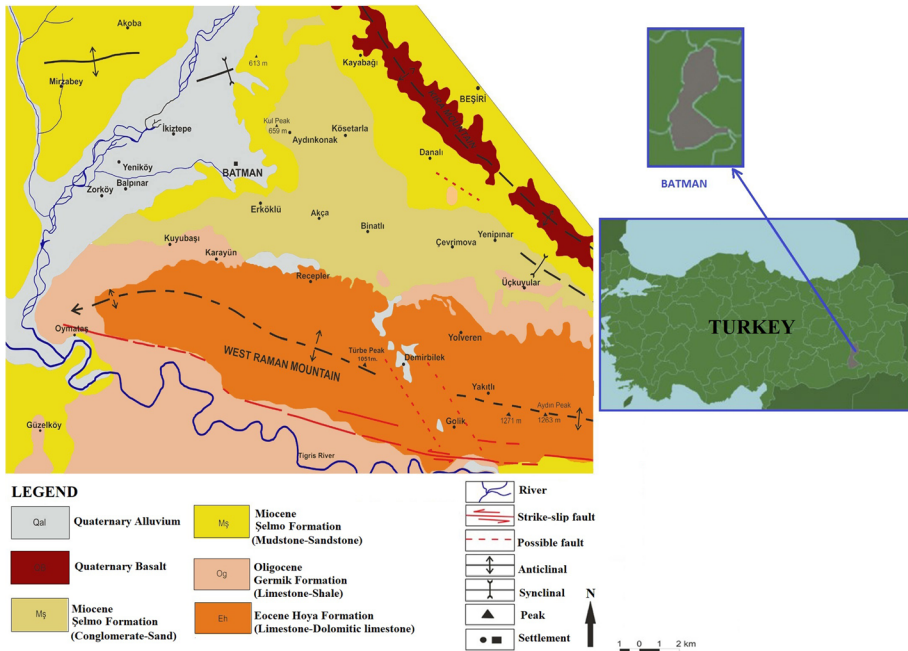


Fig. 8 Geologic map of Batman City and surrounding area, modified from The Institute of Mineral Research and Exploration (MTA) 1:500,000 scale geological map (Sunkar and Tonbul 2013)

3.1 Seismotectonics and seismic hazard of the study area

The study area and its immediate surroundings are located to the south of the “trigger zone” or contact zone of many earthquakes that occur in Türkiye. In the study area, located to the south of the edge fold region, there are parallel and regular fold areas that occur as a result of north–south directional compression movement. In order to understand the geological features of the study area, it is necessary to understand the relationship between the Anatolian Plate and the Arabian Plate, which greatly affects the geological structure of the region, and to discuss the tectonic features of a more extensive area. The Southeastern Anatolia Region and its surroundings, where the study area is located, are sheared by the East Anatolian Fault Zone (EAFZ), the Bitlis-Zagros Suture Zone (BZSZ), and the Dead Sea Fault Zone, which are among the largest tectonic structures of Türkiye, and by smaller conjugated faults of those major faults (İmamoğlu and Çetin, 2007). The EAFZ, which is one of the two main fault belts that are most active in Türkiye, spans over 580 km between Karlıova and Antakya and plays an important role in the geodynamic evolution and seismicity of the region (Arpat and Şaroğlu 1972, 1975; McKenzie 1972; Seymen and Aydın 1972; Ambrasseys, 1989; Taymaz et al. 1991). The Arabian Plate collides with the Anatolian Plate along the BZSZ, which is a region of deformation, causing the Anatolian Plate to move westward (Eyidoğan 1983; Barka and Reilinger 1997). As a result of the African-Arabian and Eurasian plates approaching each other on the north–south line, the ancient Tethys Sea, which is considered to have been the ancient ancestor of the Mediterranean, was closed off in the Lower-Middle Maastrichtian period. Following this, the Eurasian and Arabian plates collided along the Southeast Anatolian Thrust or BZSZ in the Tortonian

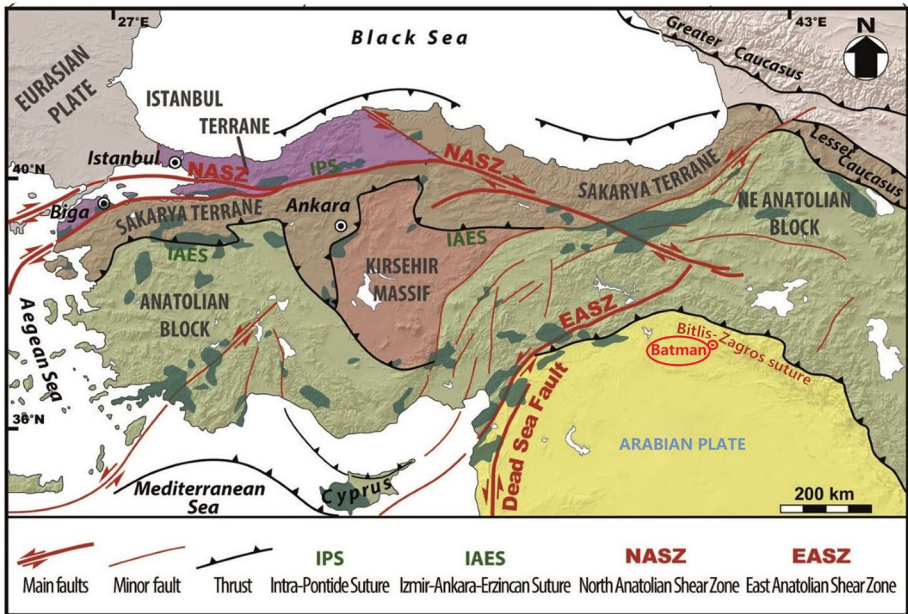


Fig. 9 NAFZ, EAFZ, Massives, Terranes, BZKK, and other important tectonic structures in the Geology of Turkey (adopted from Marroni et al. 2020)

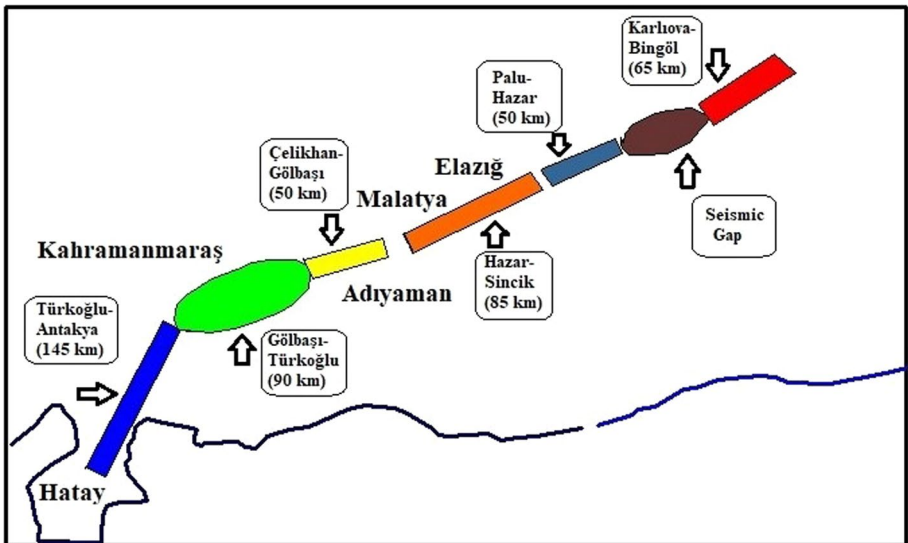


Fig. 10 Eastern Anatolian Fault Zone segments (adopted from Demirtaş and Erkmen 2019)

period, about 10 million years ago (Şengör, 1980). The Anatolian Plate moved west under the influence of the left-lateral strike-slip EAFZ and the right-lateral North Anatolian Fault Zone (NAFZ) (Barka and Kadinsky-Cade 1988; Şaroğlu et al. 1992) (Fig. 9). The East

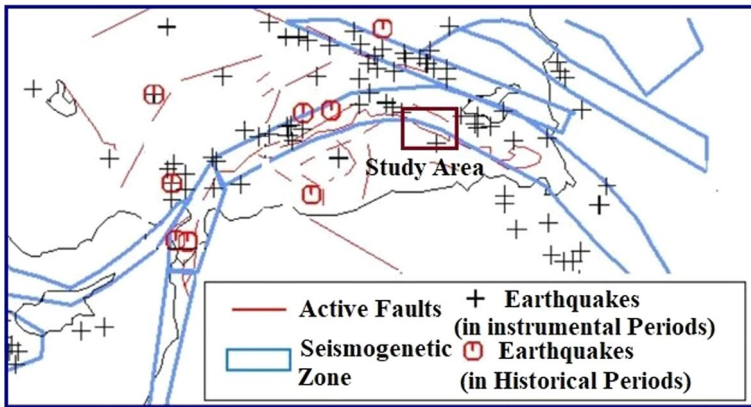


Fig. 11 Active fault zones, earthquakes in historical and instrumental periods near study area (map is redrawn by Erdik et al 1999)

Table 4 Selected fault model (A: fault rupture length is 16 km) within East Anatolian Fault Zone

Fault rupture & magnitude relation (A Model)

Fault Rupture (km) 16

Researcher	Ms (magnitude)	Conditions	Region	Magnitude type
Ambraseys and Zatopek (1969)	6.7	Between 5.8 and 8.0	Turkey	Ms
Douglas and Ryall (1975)	6.5	Bigger than 6,4	Nevada	Ms
Matsuda (1975)	6.8	–	Japan	Ms
Patwardan et al. (1975)	6.5	Bigger than 6	–	Ms
Toksöz et al. (1979)	6.2	Between 5.9 and 7.9	North Anatolia	Ms
Gündoğdu (1986)	6.4	–	Turkey	Ms
Wells ve Coppersmith (1994)	6.5	(Strike Slip)	World	Mw

Anatolian Fault (EAF) starts from the Karlıova junction point in the northeast and continues toward the Türkoğlu junction in the southwest. The EAFZ starts from the Karlıova triple junction with the NAFZ in the north and connects to the Dead Sea Fault System in the SW. The length of the EAFZ, the general direction of which is NE-SW, is about 580 km. The EAFZ is a left-lateral strike-slip fault and consists of 6 segments (Fig. 10) (Şaroğlu et al. 1992a)

Deterministic and probabilistic approaches are used to conduct seismic hazard analyses, especially in the case of developing ground movements. Seismic hazard analysis is defined as the determination of ground movements caused by earthquakes in a certain location and time period (Erdik et al. 1999). Deterministic and probabilistic approaches are widely used for the definition and evaluation of ground motion. Earthquake hazards calculated deterministically represent the level of ground movement that the largest earthquake that may occur in a region will create regardless of the time dimension (Seismic Microzonation for Municipalities: Manual, 2004). The active fault zones near the study area and relevant earthquakes in historical and instrumental periods are shown in Fig. 11. For deterministic seismic hazard analysis, two fault models within the EAFZ, namely the A fault

Table 5 Selected fault model (A: fault rupture length is 120 km) within East Anatolian Fault Zone.

FAULT RUPTURE & MAGNITUDE RELATION (B Model)				
Fault Rupture (km) 120				
Researcher	Ms (magnitude)	Conditions	Region	Magnitude type
Ambraseys and Zatopek (1969)	7.5	between 5.8 and 8.0	Turkey	Ms
Douglas and Ryall (1975)	7.5	bigger than 6.4	Nevada	Ms
Patwardan et al. (1975)	7.4	bigger than 6	–	Ms
Tocher (1958)	7.7	smaller than 6	–	Ms
Toksöz et al. (1979)	7.3	between 5.9 and 7.9	North Anatolia	Ms
Gündoğdu (1986)	7.4	–	Turkey	Ms
Wells and Coppersmith (1994)	7.5	(Strike Slip)	World	Mw

(fault rupture is 16 km) and B fault (fault rupture is 120 km), were selected (Table 4 and Table 5). The levels of ground motion for magnitudes of 7.5 and 6.5 are shown in Table 6. Table 6 also provides estimated accelerations for the region, calculated using several different attenuation relationships. It is analyzed that the results calculated for the region support each other.

3.2 Geotechnical investigation

For soil liquefaction analyses in the city center of Batman, where the study area is located, 4 boreholes were drilled in 2 locations, namely the Meydan and Bahçelievler sites, and MASW measurement studies were carried out for 4 profiles (Fig. 12). It is thought that these areas selected in the city center of Batman have high liquefaction potentials. Figure 13 shows a general view of the study area. The boreholes drilled in the Meydan site (BH-1 and BH-2) are in an area composed of low-medium plasticity clay (CL) at a depth of 1.5–3 m and one of silty sand (SM) at a depth of 3.5–12.45 m, respectively. The boreholes drilled in the Bahçelievler site (BH-3 and BH-4), on the other hand, are in an area composed of low-medium plasticity clay (CL) at a depth of 1.5–7 m and one of silty sand (SM) at a depth of 7–15 m, respectively. As can be seen in Fig. 14 a, b, according to the results obtained from these boreholes, the soils of the region can be classified mainly as low-medium plasticity clay (CL) and silty sand (SM). The SPT values obtained from the boreholes in the study area are 11–18 for the Meydan site at a depth of approximately 3.0–12.00 m and 6–18 for the Bahçelievler site (Fig. 15) at a depth of approximately 7.0–15.00 m. It was further determined that, at a depth of 3–12 m, the average gravel content is 1.3%, sand content is 68.1%, the fine grain ratio (silt + clay) is 30.6%, and PI = 14.4% at the Meydan site. At a depth of 7–15 m, the average gravel content is 1.4%, sand content is 70.2%, the fine grain ratio (silt + clay) is 28.4%, and PI = 15.3% at the Bahçelievler site. According to seismic refraction and MASW test results, Vs values fall within the range of 175–201 m/s at a depth of 3–12 m at the Meydan site and a range of 175–242 m/s at a depth of 3–12 m at the Bahçelievler site (Fig. 15).

Table 6 Ground motion level for magnitude 7.5 and 6.5

Parameter	Attenuation relationships for peak ground acceleration (PGA)									
	Δ , Epicentral distance (km)	H, Focal depth (km)	Kanai (1966)	Esteva and Vil-laverde (1973)	Abrahamson and Litehiser (1989)	Campbel (1997)	Gülkan and Kalkan (2002)	Ulusay et al. (2004)	Ulutas and Ozer (2010)	Average (g)
7.5	25	15	0.38	0.48	0.27	0.46	0.23	0.35	0.22	0.34
7.5	30	15	0.32	0.43	0.25	0.41	0.21	0.32	0.20	0.30
6.5	35	15	0.27	0.38	0.22	0.38	0.14	0.14	0.09	0.23
6.5	10	15	0.16	0.31	0.27	0.30	0.27	0.24	0.19	0.24

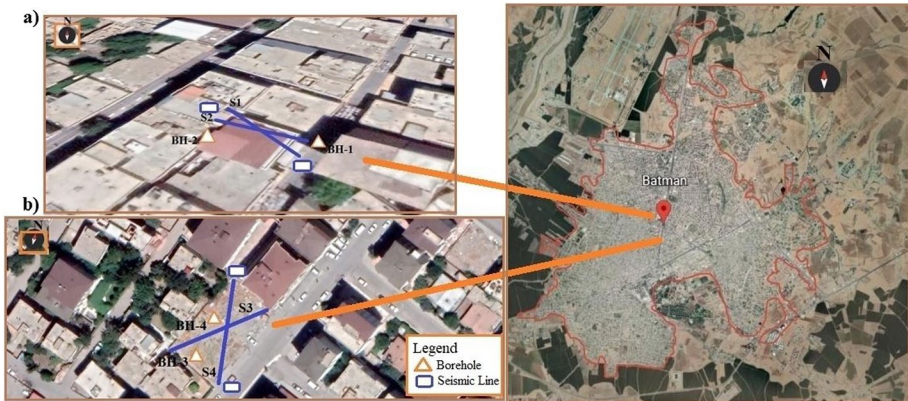


Fig. 12 Location of study area **a** Meydan and **b** Bahçelievler site drillings and seismic profile

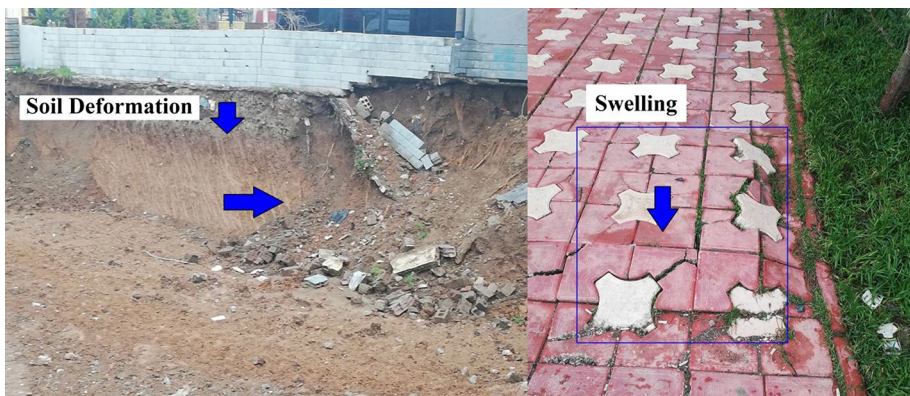


Fig. 13 General views from the study site

4 Results and discussions

In the present study, in order to observe the effects of soil and earthquake parameters on soil liquefaction, the SPT and Vs methods and the Microsoft Excel-based SoilEngineering program (Özçep, 2010) were used to make the application of liquefaction analyses more practical. Subsequently, the obtained results were discussed and interpreted. Liquefaction analyses based on the SPT and Vs methods were conducted using different earthquake magnitudes, design earthquake accelerations, groundwater levels (3 and 7 m), and depths ($z=1.8, 3.3, 4.8, 6.3, 7.8, 9.3, 10.8, 12.3, 13.8, 15.3, 16.8, 18.3, 19.8, \text{ and } 21.3$ m). The data input into SoilEngineering (Özçep, 2010) for liquefaction risk analysis of the study site, namely earthquake magnitude, design earthquake acceleration, groundwater level, and short period (0.2 s) design spectral response acceleration (SDS) values, are given in Table 7. In addition, the input data used for the calculation of shear stress ($\tau_{\text{earthquake}}$) as part of the soil liquefaction analysis performed using SoilEngineering (Özçep, 2010) are given in Table 8, Table 9, Table 10, and Table 11. The values shown in bold color are program inputs. The values in bold color throughout the liquefaction analyses performed

a) BOREHOLE LOG										b) BOREHOLE LOG													
Depth (m)	Test depth (m)	Sample type	Standart Penetration Test (SPT)				Ground Water Level : 3 m				Geotechnical and Lithological Description	Depth (m)	Test depth (m)	Sample type	Standart Penetration Test (SPT)				Ground Water Level : 7 m				Geotechnical and Lithological Description
			Blow count												Blow count								
			0.15 cm	15.30 cm	30.60 cm	N ₃₀	0.15 cm	15.30 cm	30.60 cm	N ₃₀					0.15 cm	15.30 cm	30.60 cm	N ₃₀	0.15 cm	15.30 cm	30.60 cm	N ₃₀	
0.00										0.00										Vegetable Soil			
1.50										1.50													
2.00										2.00										Low-Medium Plasticity Inorganic Clay			
3.00										3.00													
4.00		SPT1	3	5	6	11				4.00		SPT1	5	7	10	17				Low-Medium Plasticity Inorganic Clay			
4.50										4.50													
5.00		SPT2	4	6	5	11				5.00		SPT2	4	6	10	16							
6.00										6.00													
6.45		SPT3	5	6	8	14				6.45		SPT3	2	2	5	7				Silty Sand			
7.00										7.00													
7.50		SPT4	5	7	7	14				7.50		SPT4	4	3	3	6							
8.00										8.00													
9.00										9.00													
9.45		SPT5	8	8	9	17				9.45		SPT5	5	4	3	7							
10.00										10.00													
10.50		SPT6	10	8	10	18				10.50		SPT6	6	6	5	11				Silty Sand			
11.00										11.00													
12.00										12.00													
12.45		SPT7	11	8	9	17				12.45		SPT7	6	7	11	18							
13.00										13.00													
13.50		SPT8	13	15	14	29				13.50		SPT8	7	8	9	17				Low-Medium Plasticity Inorganic Clay			
14.00										14.00													
15.00										15.00													
15.45		SPT9	13	20	22	42				15.45		SPT9	8	7	11	18							

Fig. 14 a Meydan and b Bahçelievler SPT results of the study site

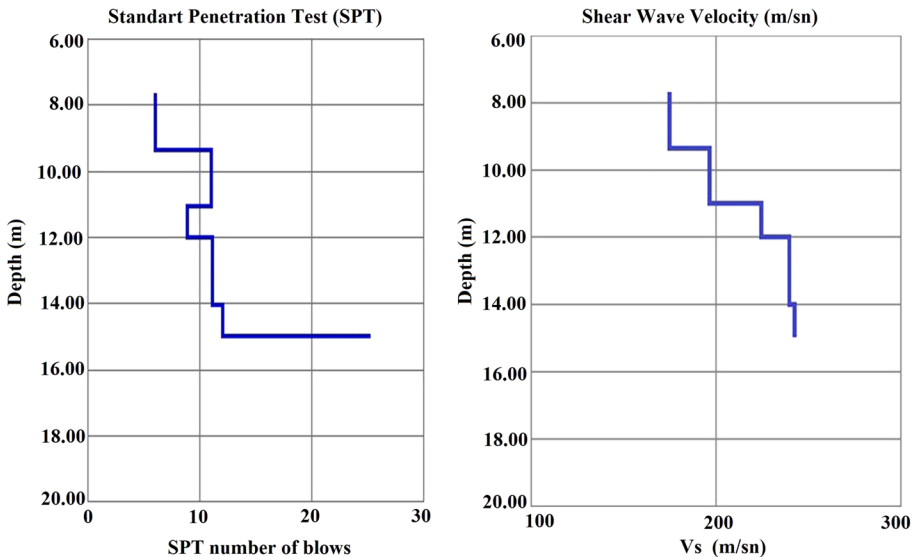


Fig. 15 Example SPT and Vs depth change for Bahçelievler site

Table 7 Earthquake and soil data set of the study area

Study site	Borehole no	Magnitude of earthquake (M)	Design earthquake acceleration (a) (g)	Ground-water (meter)	S_{DS} (Short period (0.2 s) design spectral response acceleration)
Meydan Site	BH-1	7.5	0.30	3	0.481
Meydan Site	BH-2	6.5	0.30	3	0.481
Bahçelievler Site	BH-3	7.5	0.30	7	0.697
Bahçelievler Site	BH-4	6.5	0.30	7	0.697

according to the SPT method are program inputs used for calculations of soil shear stress (τ_r). Safety factors (SF) were obtained by proportioning soil shear stress (τ_r) and earthquake shear stress ($\tau_{earthquake}$). In addition, in the analyses performed according to the Vs method, the program output states that liquefaction is not expected when the Vs1 value is theoretically greater than Vs1c (maximum: 220 m/s). The input data and SF values of calculations made according to the SPT method are presented in Table 12, Table 13, Table 14, and Table 15, respectively. The input data and SF values of calculations made according to the Vs method are presented in Table 16, Table 17, Table 18, and Table 19, respectively. In the liquefaction analysis of an earthquake of magnitude 7.5 with design earthquake acceleration of 0.30 g and a short period (0.2 s) design spectral response acceleration (SDS) of 0.481 at the BH-1 borehole in the Meydan site, where the groundwater level is 3 m, the SF values calculated for a depth of 3.3–12.3 m according to the SPT and Vs methods (Table 12 and Table 16) are 0.46–0.57 and 0.4202–0.7941, respectively. The fact that the SF values for the Meydan site are less than 1 indicates that there may be a risk of liquefaction in this area. It is seen that SF values are less than 1 in the results of both analyses. This indicates that the results support each other and the risk of liquefaction is high in this area (Fig. 16 a). In the liquefaction analysis of an earthquake of magnitude 6.5 with a design earthquake acceleration of 0.30 g and a short period (0.2 s) design spectral response acceleration (SDS) of 0.481 at the BH-2 borehole drilled in the Meydan site (Table 9), where the groundwater level is 3 m, the SF values calculated for a depth of 3.3–12.3 m according to the SPT-N method (Table 13) are 0.39–0.41 and the SF values calculated for a depth of 4.8–12.3 m according to the Vs method (Table 17) are 0.5647–0.7931. Both analyses showed that there may be a risk of liquefaction since the SF values are less than 1 at the specified depths (Fig. 16 b). In addition, analyses conducted according to the Turkish Building Earthquake Code of 2018 (Table 20) yielded results compatible with the SPT and Vs results at a depth of 4.0–12.3 m, further supporting the possibility of liquefaction.

In the liquefaction analysis of an earthquake of magnitude 7.5 with design earthquake acceleration of 0.30 g and a short period (0.2 s) design spectral response acceleration (SDS) of 0.697 at the BH-3 borehole drilled in the Bahçelievler site, where the groundwater level is 7 m, SF values calculated according to the SPT-N method are 0.33–0.75. Since the SF values calculated for liquefaction analyses according to the SPT-N method (Table 14) at a depth of 7.8–15.3 m and according to the Vs method (Table 18) at a depth of 7.8–10.8 m are less than 1, it can be concluded that there is a possible risk of liquefaction (Fig. 16 c). In the liquefaction analysis of an earthquake of magnitude 6.5 with design earthquake acceleration of 0.30 g and a short period (0.2 s) design spectral response acceleration (SDS) of 0.697 at the BH-4 borehole drilled in the Bahçelievler site, where the groundwater level is 7 m, SF values calculated for a depth of 7.8–15.8 m according to the SPT-N method (Table 15) are 0.33–0.62 while the SF values calculated for a depth of

Table 8 Input data table of SoilEngineering liquefaction analysis program for Meydan site BH-1: Cyclic shear resistance (CSR) (D) and shear stress ($\tau_{earthquake}$) results ($M_w=7.5$)

Depth (m)	Unit volume weight γ (gr/cm ³)	Fine content (FC)	Overburden pressure σ_v (kPa)	Effective overburden pressure σ'_v (kPa)	Thickness of saturated soil layer (m)	Stress reduction factor (t_d)	Cyclic stress ratio (CSR)(E)	Shear stress ($\tau_{earthquake}$)
3.3	2.01	9	65.1	62.1	0.30	0.9773893	0.213	7.9371
4.8	2.01	11	94.6	77.0	1.80	0.9669309	0.247	11.4213
6.3	2.04	14	124.7	92.3	3.30	0.9551352	0.268	14.8602
7.8	2.04	13	154.7	107.6	4.80	0.9397014	0.281	18.1405
9.3	2.04	12	184.7	122.9	6.30	0.9179441	0.287	21.1594
10.8	2.08	14	215.3	138.8	7.80	0.8875651	0.286	23.8495
12.3	2.08	15	245.9	154.7	9.30	0.8478937	0.280	26.0222

The values shown in bold color throughout the liquefaction analyses performed according to the SPT method are the program inputs used for soil shear stress ($\tau_{earthquake}$) calculations

Table 9 Input data table of SoilEngineering liquefaction analysis program for Meydan site BH-2: Cyclic shear resistance (CSR) (D) and shear stress ($\tau_{earthquake}$) results ($M_w=6.5$)

Depth (m)	Unit volume weight γ (gr/cm ³)	Fine content (FC)	Overburden pressure σ_v (kPa)	Effective overburden pressure σ'_v (kPa)	Thickness of saturated soil layer (m)	Stress reduction factor (t_d)	Cyclic stress ratio (CSR)(E)	Shear stress ($\tau_{earthquake}$)
3.3	2.02	4	65.4	62.5	0.30	0.9773893	0.213	7.9766
4.8	2.01	8	95.0	77.3	1.80	0.9669309	0.247	11.4604
6.3	2.03	7	124.8	92.5	3.30	0.9551352	0.268	14.8813
7.8	2.03	4	154.7	107.6	4.80	0.9397014	0.281	18.1440
9.3	2.03	4	184.6	122.8	6.30	0.9179441	0.287	21.1459
10.8	2.08	4	215.2	138.7	7.80	0.8875651	0.286	23.8364
12.3	2.08	5	245.8	154.6	9.30	0.8478937	0.280	26.0098

The values shown in bold color throughout the liquefaction analyses performed according to the SPT method are the program inputs used for soil shear stress ($\tau_{earthquake}$) calculations

Table 10 Input data table of SoilEngineering liquefaction analysis program for Bahçelievler site BH-3; Cyclic shear resistance (CSR) (D) and shear stress ($\tau_{earthquake}$) results ($M_w=7.5$)

Depth (m)	Unit volume weight $\gamma(g/cm^3)$	Fine content (FC)	Overburden pressure σ_v (kPa)	Effective overburden pressure σ'_v (kPa)	Thickness of saturated soil layer (m)	Stress reduction factor (r_d)	Cyclic stress ratio (CSR)(E)	Shear stress ($\tau_{earthquake}$)
7.8	1.94	5	148.4	140.6	0.80	0.9397014	0.193	25.0252
9.3	1.94	8	177.0	154.4	2.30	0.9179441	0.205	29.1469
10.8	1.94	12	205.5	168.3	3.80	0.8875651	0.211	32.7278
12.3	1.97	10	234.5	182.5	5.30	0.8478937	0.212	35.6745
13.8	1.96	7	263.4	196.7	6.80	0.8008678	0.209	37.8397
15.3	1.97	6	292.4	210.9	8.30	0.7507104	0.203	39.3740

The values shown in bold color throughout the liquefaction analyses performed according to the SPT method are the program inputs used for soil Shear stress ($\tau_{earthquake}$) calculations

Table 11 Input data table of SoilEngineering liquefaction analysis program for Bahçelievler site BH-4; Cyclic shear resistance (CSR) (D) and shear stress ($\tau_{\text{earthquake}}$) results ($M_w=6.5$)

Depth (m)	Unit volume weight γ (gr/cm^3)	Fine content (FC)	Overburden pressure σ'_v (kPa)	Effective overburden pressure σ'_v (kPa)	Thickness of saturated soil layer (m)	Stress reduction factor (r_d)	Cyclic stress Ratio (CSR)(E)	Shear stress ($\tau_{\text{earthquake}}$)
7.8	1.95	6	149.2	141.4	0.80	0.9397014	0.193	25.1542
9.3	1.95	8	177.9	155.3	2.30	0.9179441	0.205	29.2971
10.8	1.94	11	206.5	169.2	3.80	0.8875651	0.211	32.8731
12.3	1.94	10	235.0	183.0	5.30	0.8478937	0.212	35.7461
13.8	1.96	7	263.8	197.1	6.80	0.8008678	0.209	37.9074
15.3	1.97	6	292.8	211.4	8.30	0.7507104	0.203	39.4374

The values shown in bold color throughout the liquefaction analyses performed according to the SPT method are the program inputs used for soil shear stress ($\tau_{\text{earthquake}}$) calculations

Table 12 Input data table of SoilEngineering liquefaction analysis program showing standard penetration test (SPT) analysis for Meydan site BH-1: Shear resistance ratio (CRR) (Z) and safety factor (SF) results ($M_w = 7.5$)

Depth (m)	Standard Penetration Test (SPT(N) value in the field	for SPT(N) and Vs, effective pressure correction factor,(CN)	Hammer energy ratio (CE)	Borehole correction factor (CB)	Correction factor for samples (CS)	Rod length correction factor (CR)	Corrected SPT (N) value (N1(60)	Cyclic resistance ratio (CRR)(S)	Safety factor (SF)
3.3	11	1.25	0.75	1.0	1.1	0.75	9.2	0.1065	0.50
4.8	11	1.13	0.75	1.0	1.1	0.85	10.1	0.1143	0.46
6.3	14	1.03	0.75	1.0	1.1	0.85	12.7	0.1381	0.51
7.8	14	0.95	0.75	1.0	1.1	0.95	12.7	0.1380	0.49
9.3	17	0.89	0.75	1.0	1.1	0.95	13.8	0.1484	0.52
10.8	18	0.84	0.75	1.0	1.1	1.00	15.2	0.1621	0.57
12.3	17	0.80	0.75	1.0	1.1	1.00	14.2	0.1520	0.54

Standard Penetration Test (SPT) in the field and calculated Safety factor values are given in bold color

Table 13 Input data table of SoilEngineering liquefaction analysis program showing standard penetration test (SPT) analysis for Meydan site BH-2: Shear resistance ratio (CRR) (Z) and safety factor (SF) results ($M_w = 6.5$)

Depth (m)	Standard Penetration Test (SPT)(N) value in the field	for SPT(N) and V_s , effective pressure correction factor,(CN)	Hammer energy ratio (CE)	Borehole correction factor(CB)	Correction factor for samples (CS)	Rod length correction factor(CR)	Corrected SPT (N) value (N1(60))	Cyclic resistance ratio (CRR)(S)	Safety factor (SF)
3.3	4	1.25	0.75	1.0	1.1	0.75	3.1	0.0851	0.40
4.8	5	1.12	0.75	1.0	1.1	0.85	4.3	0.0965	0.39
6.3	7	1.03	0.75	1.0	1.1	0.85	5.2	0.1062	0.40
7.8	8	0.95	0.75	1.0	1.1	0.95	6.0	0.1147	0.41
9.3	9	0.89	0.75	1.0	1.1	0.95	6.3	0.1183	0.41
10.8	9	0.84	0.75	1.0	1.1	1.00	6.2	0.1176	0.41
12.3	9	0.80	0.75	1.0	1.1	1.00	5.9	0.1139	0.41

Standard Penetration Test (SPT) in the field and calculated Safety factor values are given in bold color

Table 14 Input data table of SoilEngineering liquefaction analysis program showing standard penetration test (SPT) analysis for Bahçelievler site BH-3: Shear resistance ratio (CRR) (Z) and safety factor (SF) results ($M_w = 7.5$)

Depth (m)	Standard Penetration Test (SPT)(N) value in the field	for SPT(N) and Vs, effective pressure correction factor,(CN)	Hammer energy ratio (CE)	Borehole correction factor (CB)	Correction factor for samples (CS)	Rod length correction factor (CR)	Corrected SPT (N) value (N1(60))	Cyclic resistance ratio (CRR)(S)	Safety factor (SF)
7.8	6	0.83	0.75	1.0	1.1	0.95	3.9	0.0643	0.33
9.3	11	0.80	0.75	1.0	1.1	0.95	7.2	0.0897	0.44
10.8	9	0.76	0.75	1.0	1.1	1.00	7.4	0.0909	0.43
12.3	11	0.73	0.75	1.0	1.1	1.00	7.7	0.0931	0.44
13.8	12	0.71	0.75	1.0	1.1	1.00	7.2	0.0890	0.43
15.3	25	0.68	0.75	1.0	1.1	1.00	14.1	0.1515	0.75

Standard Penetration Test (SPT) in the field and calculated Safety factor values are given in bold color

Table 15 Input data table of Soil Engineering liquefaction analysis program showing standard penetration test (SPT) analysis for Bahçelievler site BH-4; Shear resistance ratio (CRR) (Z) and safety factor (SF) results ($M_w = 6.5$)

Depth (m)	Standard Penetration Test (SPT)(N) value in the field	Correction factor for SPT(N) and Vs, effective pressure correction factor,(CN)	Hammer energy ratio (CE)	Borehole correction factor (CB)	Correction factor for samples (CS)	Rod length correction factor(CR)	Corrected SPT (N) value (N1(60))	Cyclic resistance ratio (CRR)(S)	Safety factor (SF)
7.8	6	0.83	0.75	1.0	1.1	0.95	4.0	0.0646	0.33
9.3	7	0.79	0.75	1.0	1.1	0.95	4.7	0.0699	0.34
10.8	11	0.76	0.75	1.0	1.1	1.00	8.3	0.0984	0.47
12.3	18	0.73	0.75	1.0	1.1	1.00	12.0	0.1308	0.62
13.8	17	0.70	0.75	1.0	1.1	1.00	10.1	0.1139	0.54
15.3	18	0.68	0.75	1.0	1.1	1.00	10.2	0.1147	0.57

Standard Penetration Test (SPT) in the field and calculated Safety factor values are given in bold color

Table 16 Input data table of SoilEngineering liquefaction analysis program showing shear wave velocity (V_s) analysis for Meydan site BH-1: Safety factor (SF) results ($M_w=7.5$)

Depth (m)	Shear wave velocity (Field)(V_s) (m/sn)	for SPT(N) and V_s , effective pore correction factor,(CV)	Corrected shear wave velocity (V_{s1}) (m/sn)	Corrected shear wave velocity (V_{sc1})(m/sn)	Cyclic resistance ratio (CRR)(z)	Safety factor (SF)
3.3	173	1.13	194.86	210	0.1691	0.7941
4.8	176	1.07	187.89	210	0.1423	0.5757
6.3	181	1.02	184.67	210	0.1335	0.4976
7.8	191	0.98	187.54	210	0.1413	0.5028
9.3	191	0.95	181.40	210	0.1259	0.4388
10.8	194	0.92	178.74	210	0.1203	0.4202
12.3	200	0.90	179.34	210	0.1215	0.4335

Shear wave velocity (V_s) measured in the field and calculated Safety factor values are in bold color

Table 17 Input data table of SoilEngineering liquefaction analysis program showing shear wave velocity (V_s) analysis for Meydan site BH-2; Safety factor (SF) results ($M_w=6.5$)

Depth (m)	Shear wave velocity (Field)(V_s) (m/sn)	for SPT(N) and V_s , effective pressure correction factor,(CV)	Corrected shear wave velocity (V_{s1}) (m/sn)	Corrected shear wave velocity (V_{sc1}) (m/sn)	Cyclic resistance ratio (CRR)(z)	Safety factor (SF)
3.3	175	1.12	196.86	220	0.2179	1.0236
4.8	174	1.07	185.56	210	0.1959	0.7931
6.3	179	1.02	182.54	210	0.1853	0.6908
7.8	180	0.98	176.72	220	0.1592	0.5668
9.3	191	0.95	181.45	220	0.1702	0.5931
10.8	193	0.92	177.85	220	0.1618	0.5647
12.3	201	0.90	180.27	220	0.1674	0.5969

Shear wave velocity (V_s) measured in the field and calculated Safety factor values are in bold color

Table 18 Input data table of SoilEngineering liquefaction analysis program showing shear wave velocity (Vs) analysis for Bahçelievler site BH-3; Safety factor (SF) results ($M_w=7.5$)

Depth (m)	Shear wave velocity (Field)(Vs) (m/sn)	for SPT(N) and Vs, effective pres-sure correction factor,(CV)	Corrected shear wave velocity (Vs1) (m/sn)	Corrected shear wave velocity (Vsc1) (m/sn)	Cyclic resistance ratio (CRR)(z)	Safety factor (SF)
7.8	175	0.92	160.71	220	0.0886	0.4578
9.3	196	0.90	175.82	210	0.1148	0.5595
10.8	224	0.88	196.68	210	0.1793	0.8481
12.3	238	0.86	204.76	210	0.2932	1.3801
13.8	240	0.84	202.67	210	0.2417	1.1555
15.3	241	0.83	199.98	210	0.2055	1.0127

Shear wave velocity (Vs) measured in the field and calculated Safety factor values are in bold color

Table 19 Input data table of SoilEngineering liquefaction analysis program showing shear wave velocity (V_s) analysis for Bahçelievler site BH-4: Safety factor (SF) results ($M_w=6.5$)

Depth (m)	Shear wave velocity (Field)(V_s) (m/sn)	for SPT(N) and V_s , effective pressure correction factor,(CV)	Corrected shear wave velocity (V_{s1}) (m/sn)	Corrected shear wave velocity (V_{sc1}) (m/sn)	Cyclic resistance ratio (CRR)(z)	Safety factor (SF)
7.8	175	0.92	160.49	210	0.0912	0.4714
9.3	192	0.90	171.98	210	0.1081	0.5274
10.8	223	0.88	195.53	210	0.1726	0.8173
12.3	221	0.86	190.01	210	0.1490	0.7020
13.8	231	0.84	194.95	210	0.1695	0.8111
15.3	242	0.83	200.69	210	0.2133	1.0518

Shear wave velocity (V_s) measured in the field and calculated Safety factor values are in bold color

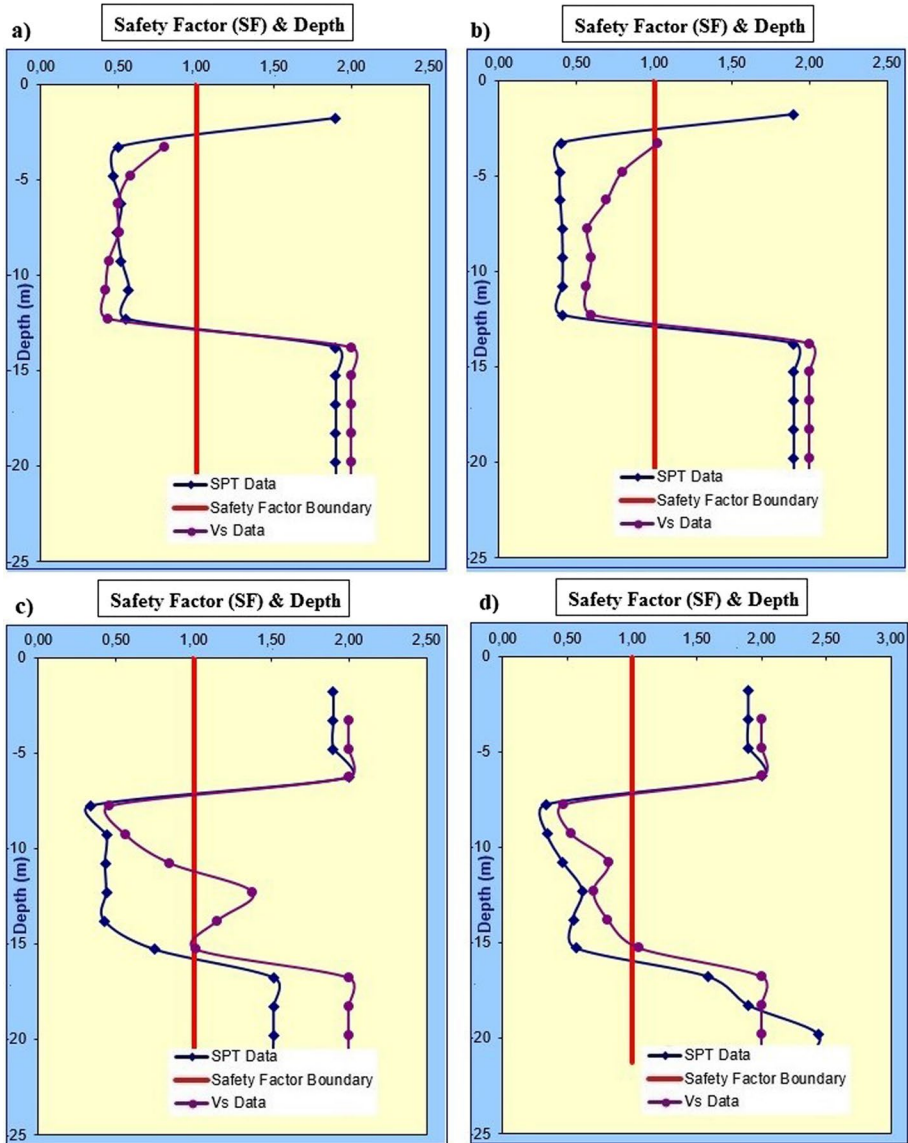


Fig. 16 a Meydan site (BH-1) b Meydan site (BH-2)–4 c Bahçelievler site (BH-3) d Bahçelievler site (BH-4). Safety factor (SF) and depth change graphs according to standard penetration test (SPT) and shear wave velocity (Vs) data

7.8–13.8 m according to the Vs method (Table 19) are 0.4714–0.8173. Thus, the results of liquefaction analysis performed according to the Vs method suggest a risk of liquefaction at depths between roughly 7 m and 13 m, with no risk of liquefaction at deeper depths (Fig. 16 d). In addition, analyses performed according to the Turkish Building Earthquake Code of 2018 (Table 21) yielded results compatible with the SPT and Vs results at a depth of 7.0–14.0 m, supporting the possibility of liquefaction.

Table 20 According to Turkish Building Earthquake Regulations (2018), liquefaction risk analysis of Meydan site (BH-1 and BH-2) Safety Factor (SF) values

Meydan site BH-1 depth (m)	Turkish building earthquake regulations (2018) safety factor (SF)	Meydan site BH-2 depth (m)	Turkish building earthquake regulations (2018) safety factor (SF)
3.3	0.83	3.3	0.96
4.8	0.77	4.8	0.94
6.3	0.86	6.3	0.95
7.8	0.82	7.8	0.98
9.3	0.86	9.3	0.99
10.8	0.94	10.8	0.99
12.3	0.90	12.3	0.98

Safety factor (SF) values calculated according to the Turkish Building Earthquake Code (2018) are given in bold color

Table 21 According to Turkish Building Earthquake Regulations (2018), liquefaction risk analysis of Bahçelievler site (BH-3 and BH-4) Safety Factor (SF) values

Bahçelievler site BH-3 depth (m)	Turkish building earthquake regulations (2018) safety factor (SF)	Bahçelievler site BH-4 Depth (m)	Turkish building earthquake regulations (2018) safety factor (SF)
7.8	0.36	7.8	0.36
9.3	0.47	9.3	0.37
10.8	0.47	10.8	0.51
12.3	0.48	12.3	0.67
13.8	0.46	13.8	0.59
15.3	0.81	15.3	0.61

Safety factor (SF) values calculated according to the Turkish Building Earthquake Code (2018) are given in bold color

Table 22 Changes in the depth and settlement for study area

Depth (m)	Meydan site BH-1 Total settlement (cm)	Meydan site BH-2 Total settlement (cm)	Bahçelievler site BH-3 Total settlement (cm)	Bahçelievler site BH-4 Total settlement (cm)
	32.06	49.8	36.87	36.2
1.8	0.00	0.00	0.00	0.00
3.3	5.53	8.20	0.00	0.00
4.8	5.21	7.60	0.00	0.00
6.3	4.50	7.14	0.00	0.00
7.8	4.50	6.76	7.79	7.77
9.3	4.21	6.64	6.28	7.40
10.8	3.98	6.66	6.23	5.89
12.3	4.13	6.80	6.13	4.71
13.8	0.00	0.00	6.31	5.23
15.3	0.00	0.00	4.13	5.20

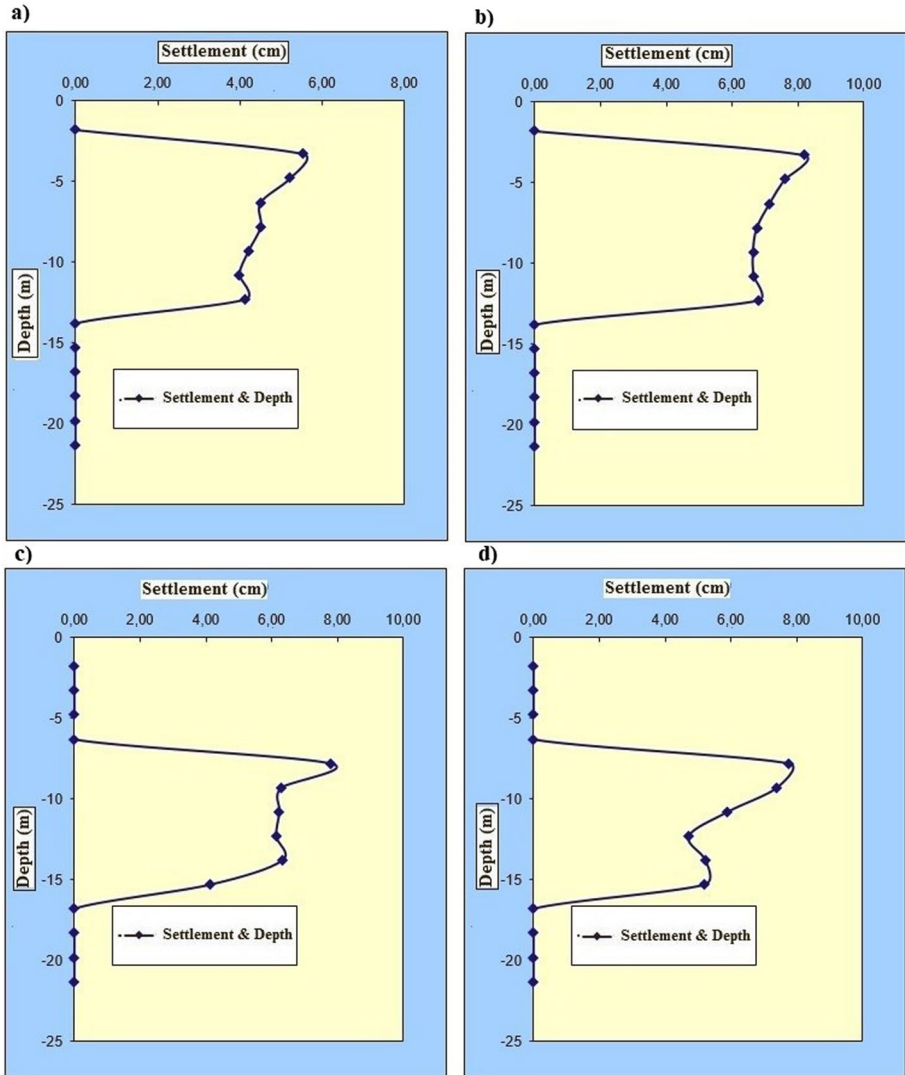


Fig. 17 Graphs of changes in depth and settlement amounts in **a** Meydan site (BH-1) **b** Meydan site (BH-2) **c** Bahçelievler site (BH-3) **d** Bahçelievler site (BH-4)

Recompression settlement following liquefaction in sand units can occur very quickly with the sudden damping of the pore water pressure due to dynamic loads. Sands tend to be compacted underground due to earthquake tremors and their underground compaction tendency manifests itself on the surface in the form of soil settlement. In this study, surface settlement amounts resulting from vertical strain due to excess pore water pressure being damped were calculated by multiplying and integrating the volumetric strain value [ev (%)] obtained for

each depth at the study site with the depth for which they were obtained and then superposing the results (Ishihara and Yoshimine 1992). As can be seen in Table 22, in the analyses conducted for the BH-1 and BH-2 boreholes drilled in the Meydan site, total settlement amounts of 32.06 cm and 49.8 cm were calculated respectively for depths of 3.3–12.3 m, and in the analyses conducted for the BH-3 and BH-4 boreholes drilled in the Bahçelievler site, total settlement amounts of 36.87 cm and 36.2 were respectively calculated for depths of 7.8–15.3 m. Liquefaction potential is high for the boreholes drilled in the Meydan site (BH-1 and BH-2) at depths of roughly 3.3–12.3 m, and accordingly, there may be high amounts of settlement in the soil layers at these depths (Fig. 17a, b). Liquefaction potential observed for the boreholes drilled in the Bahçelievler site (BH-3 and BH-4) at depths of roughly 7.8–15.3 m was also supported by the high amount of soil settlement at those depths (Fig. 17c, d).

5 Conclusions

In this study, in order to determine soil liquefaction potential in the residential area of Batman Province, located in the Southeastern Anatolia Region of Türkiye, 4 boreholes were drilled in 2 locations, namely the Meydan and Bahçelievler sites, and MASW measurement studies were carried out for 4 profiles. To determine the risk of soil liquefaction, which is one of the most important sources of damage caused by earthquakes to structures in residential areas, a series of analyses based on SPT and Vs data were performed. Within the scope of the research, SPT and Vs parameters obtained from field studies were analyzed together with earthquake parameters in order to obtain SF values reflecting the risk of liquefaction. These SF values were then interpreted and presented. In addition, all obtained results were compared and evaluated in accordance with the SF results calculated for liquefaction risk according to the Turkish Building Earthquake Code of 2018. Analyses of liquefaction risk and liquefaction-related settlement, which are crucial soil problems in geotechnical engineering, were conducted using the computer-aided SoilEngineering program (Özçep, 2010), which provides collective calculation methods and visual graphics. It was found that all analyses performed to determine liquefaction potentials supported each other. Thus, calculating the liquefaction risk according to both soil and earthquake characteristics in future studies will provide more useful and reliable results in solving geotechnical problems.

Liquefaction analyses were carried out in this study using design earthquake features with magnitudes of 7.5 and 6.5, reflecting the earthquakes that may be produced within the EAFZ located close to the study area. In the liquefaction analysis of an earthquake of magnitude 7.5 with design earthquake acceleration of 0.30 g and a short period (0.2 s) design spectral response acceleration (SDS) of 0.481 for the BH-1 borehole drilled in the Meydan site, where the groundwater level is 3 m, the SF values calculated for a depth of 3.3–12.3 m according to the SPT and Vs methods were smaller than 1. This indicates a potential for liquefaction in the area. In the liquefaction analysis performed for an earthquake with magnitude of 6.5, design earthquake acceleration of 0.30 g, and a short period (0.2 s) design spectral response acceleration (SDS) of 0.481 for the BH-2 borehole in the Meydan site, where the groundwater level is 3 m, the SF values calculated for a depth of 3.3–12.3 m according to the SPT-N method were 0.39–0.41, while the SF values calculated for a depth of 4.8–12.3 m according to the Vs method (Table 17) were 0.5647–0.7931. Both sets of analyses showed that there may be a risk of liquefaction since the SF values were smaller than 1 at the specified depths. In addition, analyses performed according to the Turkish

Building Earthquake Code of 2018 yielded results compatible with the SPT and V_s data at a depth of 4.0–12.3 m, supporting the possibility of liquefaction.

In the liquefaction analysis performed for an earthquake of magnitude 7.5 with design earthquake acceleration of 0.30 g and a short period (0.2 s) design spectral response acceleration (SDS) of 0.697 for the BH-3 borehole drilled in the Bahçelievler site, where the groundwater level is 7 m, the SF values calculated for liquefaction analyses using the SPT-N method at a depth of 7.8–15.3 m and the V_s method at a depth of 7.8–10.8 m were smaller than 1. Thus, it can be concluded that there is a risk of liquefaction. In the liquefaction analysis for an earthquake of magnitude 6.5 with design earthquake acceleration of 0.30 g and a short period (0.2 s) design spectral response acceleration (SDS) of 0.697 for the BH-4 borehole drilled in the Bahçelievler site, where the groundwater level is 7 m, liquefaction risks were observed at a depth of 7.8–15.8 m according to the SPT-N method and a depth of roughly 7–13 m according to the V_s method, while no risk of liquefaction was seen at deeper depths. In addition, analyses performed according to the Turkish Building Earthquake Code of 2018 yielded results compatible with the SPT and V_s results at a depth of 7.0–14.0 m, supporting the possibility of liquefaction.

Furthermore, the liquefaction risk indices of the studied zone obtained by the SPT method and those obtained by the V_s method were found to be compatible with each other. Liquefaction analyses were conducted with SPT data for areas of Batman Province with liquefaction potential under the conditions of earthquake moment magnitude of $M_w = 7.5$ and $M_w = 6.5$ and design earthquake acceleration of 0.30 g, which could be produced by future earthquakes occurring due to the rupture of the EAFZ. Finally, it was determined that there may be large amounts of settlement in soil layers where the liquefaction risk potential is high.

Authors contributions All authors contributed jointly in creating the dataset, using the computer program, and performing the calculations. All authors contributed to the preparation, writing, and editing of the manuscript.

Funding No funding was received for this publication.

Data availability The data analyzed for this article are available within the article and in its online supplementary material.

Declarations

Conflict of interest The authors declare that they have no conflict of interest.

References

- Abrahamson NA, Litehiser JJ (1989) Attenuation of vertical peak acceleration. *BSSA* 79(3):549–580. <https://doi.org/10.1785/BSSA0790030549>
- Açıkbaş D, Baştuğ C (1975) Geological report and oil possibilities of the northern fields of Cacas-Hani region, Region V, TPAO Exploration Group, Report no. 917: 45, Ankara
- Akın KM, Kramer SL, Topal T (2011) Empirical correlations of shear wave velocity (V_s) and penetration resistance (SPT-N) for different soils in an earthquake-prone area (Erbaa-Turkey). *Eng Geol* 119(1–2):1–17. <https://doi.org/10.1016/j.enggeo.2011.01.007>
- Akkaya İ, Özvan A, Akın M, Akın MK, Övün U (2018) Comparison of SPT and V_s -Based liquefaction analyses: a case study in Erciş (Van, Turkey). *Acta Geophys* 66:21–38. <https://doi.org/10.1007/s11600-017-0103-0>

- Ambraseys NN (1988) Engineering seismology. *Earthquake Eng Struct Dynam* 17(1):1–105. <https://doi.org/10.1002/eqe.4290170102>
- Ambraseys NN (1989) Temporary seismic quiescence: SE Turkey. *Geophys J* 96:311–331. <https://doi.org/10.1111/j.1365-246X.1989.tb04453.x>
- Ambraseys NN, Zapotek A (1969) The Mudurnu valley (West Anatolia, Turkey) earthquake of 22 July 1967. *Bull Seis Soc* 59(2):521–589. <https://doi.org/10.1785/BSSA0590020521>
- Andrus RD, Stokoe KH II (2000) Liquefaction resistance of soils from shear wave velocity. *J Geotech Geoenviron Eng* 126(11):1015–1025. [https://doi.org/10.1061/\(ASCE\)1090-0241\(2000\)126:11\(1015\)](https://doi.org/10.1061/(ASCE)1090-0241(2000)126:11(1015))
- Arpat E, Saroglu F (1972) The East anatolian fault system: thoughts on its development *M.T.A. Bull* 78:33–39
- Arpat E, Saroglu F (1975) Türkiye'deki bazı önemli genc tektonik olaylar. *Bull Geol Soc Turkey* 18(1):91–101 (**in Turkish**)
- Barka AA, Kadinsky-Cade K (1988) Strike-slip fault geometry in Turkey and its fluence on earthquake activity. *Tectonics* 7(3):663–684. <https://doi.org/10.1029/TC007i003p00663>
- Barka A, Reilinger R (1997) Active tectonics of the Eastern Mediterranean region: deduced from GPS, neotectonic and seismicity data. *Ann Geofis* 2(3):587–610
- Bekin E, Özçep F (2021) A comparative soil liquefaction analysis with a MATLAB® based algorithm: soil-Lique. *Earth Sci Res J* 25(3):323–340. <https://doi.org/10.15446/esrj.v25n3.86525>
- Bolgi T (1961) V. Petrol Bölgesi seksiyon ölçümleri AR/TPO/261 nolu saha ile Reşan Dodan arası batısındaki sahanın strüktürel etüdüleri, TPAO Arama Grubu Rapor No. 162, Ankara (**in Turkish**)
- Boulanger RW, Idriss IM (2014) CPT and SPT based liquefaction triggering procedures. Report No. UCD/CGM.-14, 1
- Campbell KW (1997) Empirical near-source attenuation relationships for horizontal and vertical components of peak ground acceleration, peak ground velocity, and pseudo-absolute acceleration response spectra. *Seismol Res Lett* 68(1):154–179. <https://doi.org/10.1785/gssrl.68.1.154>
- Castro G (1969) Liquefaction of sands, Harvard Soil Mechanics Series, 81. Pierce Hall, Cambridge, Massachusetts
- Çetin KO, Seed RB (2004) Nonlinear shear mass participation factor (rd) for cyclic shear stress ratio evaluation. *Soil Dyn Earthq Eng* 24:103–113. <https://doi.org/10.1016/j.soildyn.2003.10.008>
- Dadashpour M, Echeverria-Ciaurri D, Kleppe J, Landro M (2009) Porosity and permeability estimation by integration of production and time-lapse near and far offset seismic data. *J Geophys Eng* 6:325–344. <https://doi.org/10.1088/1742-2132/6/4/001>
- Demirtas R, Erkmen C (2019) Eastern Anatolia fault system earthquake activity. *Future Earthquake Potential Res.* <https://doi.org/10.13140/RG.2.2.24235.49449>
- Dobry R, Stokoe KHII, Ladd RS, Youd TL (1981) Liquefaction susceptibility from S-Wave Velocity. In: *Proceedings, In Situ Tests to Evaluate Liquefaction Susceptibility*, ASCE National Convention, St. Louis, MO
- Douglas MB, Ryal LA (1975) Return periods for rock acceleration in western Nevada. *BSSA* 65:1599–1611. <https://doi.org/10.1785/BSSA0650061599>
- Duan W, Zhao Z, Cai G et al (2023) V_s -based assessment of soil liquefaction potential using ensemble of GWO–KLEM and Bayesian theorem: a full probabilistic design perspective. *Acta Geotech* 18:1863–1881. <https://doi.org/10.1007/s11440-022-01695-2>
- Erdik M, Alpaly T, Biro Y, Onur T, Sesettyan K, Birgoren G (1999) Assessment of earthquake hazard in Turkey and neighboring regions. *Ann Geofis* 42:1125–1138
- Eren Y, Nalbantçılar MT, Beyaz T, Dinç S, Ünal M, Arslan Ş, Polat S (2012) Tectonism of Esentepe (Gültepe/Batman) Hole. *Batman Univ J Life Sci* 1(2):385–394
- Esteva L, Villaverde R (1973) Seismic risk, design spectra and structural reliability. In: *Proceedings of fifth world conference on earthquake engineering*, vol 2, pp 2586–2596
- Eyidoğan H (1983) Bitlis-Zağros bindirme ve kıvrımlı kuşağının sismotektonik özellikleri. *Doktora Tezi, İstanbul Teknik Üniversitesi, Maden Fakültesi*, 112s (yayımlanmamış) (**in Turkish**)
- Eyisüren O, Karaca Ö, Büyüksaraç A, Işık E (2023) Combined use of standard penetration test and shear wave velocities in liquefaction analysis: Çanakkale example. In: Ademović N, Mujić E, Mulić M, Kevrić J, Akšamija Z (eds) *Advanced technologies, systems, and applications VII*. IAT 2022 Lecture notes in networks and systems. Springer, Cham. https://doi.org/10.1007/978-3-031-17697-5_5
- Gülkan P, Kalkan E (2002) Attenuation modelling of recent earthquake in Turkey. *J Seismolog* 6:397–409. <https://doi.org/10.1023/A:1020087426440>
- Idriss IM, Boulanger RW (2008) Soil liquefaction during earthquakes. Earthquake Engineering Research Institute, EERI Publication, Monograph MNO-12, Oakland, CA
- Idriss IM, Boulanger RW (2010) SPT-based liquefaction triggering procedures. Rep. UCD/CGM-10, 2, 4-13

- Idriss IM (1999) An update to the Seed-Idriss simplified procedure for evaluating liquefaction potential. In: Proceedings of TRB Workshop on New Approaches to Liquefaction, Federal Highway Administration, Washington, DC
- Ishihara K, Yoshimine M (1992) Evaluation of settlements in sand deposits following liquefaction during earthquakes. *Soils Found* 32(1):173–188. <https://doi.org/10.3208/sandf1972.32.173>
- Kanai K (1966) Observation Of Microtremor, Xi., Matsushiro Earthquake Swarm Areas, Bulletin Of Earthquake Research Institute, Xliv, part 3, University Of Tokyo
- Karakas A, Coruk O (2010) Liquefaction analysis of soils in the Western Izmit Basin Turkey. *Environ Eng Geosci* 16(4):411–430. <https://doi.org/10.2113/gseengeosci.16.4.411>
- Kayen R, Moss RES, Thompson EM, Seed RB, Cetin KO, Kiureghian AD et al (2013) Shear-wave velocity-based probabilistic and deterministic assessment of seismic soil liquefaction potential. *J Geotech Geoenviron Eng* 139(3):407–419. [https://doi.org/10.1061/\(ASCE\)GT.1943-5606.0000743](https://doi.org/10.1061/(ASCE)GT.1943-5606.0000743)
- Kishida H (1969) Characteristics of liquefied sands during Mino-Owari, Tohankai and Fukui earthquakes. *Soils Found* 9(1):75–92. <https://doi.org/10.3208/sandf1960.9.75>
- Koc G (2007) Evaluation of the liquefaction potential of Gölcük and its Region. Kocaeli University Graduate School of Natural Appl Sci, Kocaeli
- Kramer SL (1996) Geotechnical earthquake engineering. Prentice-Hall Inc, USA, pp 1–653
- Lambe PC (1981) Dynamic centrifuge modelling of a horizontal sand stratum. Sc.D thesis, Massachusetts Institute of Technology
- Liao SSC, Whitman RV (1986) Overburden correction factors for SPT in sand. *J Geotech Eng* 112(3):373–377. [https://doi.org/10.1061/\(ASCE\)0733-9410\(1986\)112:3\(373\)](https://doi.org/10.1061/(ASCE)0733-9410(1986)112:3(373))
- Marroni M, Göncüoğlu MC, Frassi C, Sayit K, Pandolf L, Ellero A, Ottria G (2020) The Intra-Pontide ophiolites in Northern Turkey revisited: from birth to death of a Neotethyan oceanic domain. *Geosci Front* 11(1):129–149. <https://doi.org/10.1016/j.gsf.2019.05.010>
- Matsuda T (1975) Magnitude and recurrence interval of earthquake from a fault. *J Seismol Soc Japan (ZISIN)* 28:269–283 (in Japanese with English)
- McKenzie DP (1972) Active tectonics of the Mediterranean Region. *Geophys J R Astron Soc* 30(109–185):1972. <https://doi.org/10.1111/j.1365-246X.1972.tb02351.x>
- Turkish Building Earthquake Code (TBEC 2018) (2018) Ministry of public works and settlement. Specification for structures to be built in disaster areas. Government of the Republic of Turkey. *Official Gazette*, No: 30364
- Onalp A (1983) Geotechnical Information for Civil Engineers. Vol. II, Karadeniz University Edition No: 3, Trabzon, 1225
- Ozcep F, Zarif H (2009) Variations of soil liquefaction safety factors depending on several design earthquakes in the city of Yalova (Turkey). *Sci Res Essays* 4(6):594–604
- Ozcep F, Aşti M, Karabulut S, Alpaslan N, Yas T (2003) Evaluation of liquefaction potential of soils by different methods. *Appl Earth Sci* 3(2):11–22
- Ozcep F (2010) Soil engineering: a Microsoft Excel (R) spreadsheet (c) program for geotechnical and geophysical analysis of soils. *Comput Geosci* 36(10):1355–1361. <https://doi.org/10.1016/j.cageo.2010.01.015>
- Ozcep F, Karabulut S, Ozel O, Ozcep T, Imre N, Zarif H (2014) Liquefaction-induced settlement, site effects and damage in the vicinity of Yalova City during the 1999 Izmit earthquake. *Turkey J Earth Syst Sci* 123(1):73–89. <https://doi.org/10.1007/s12040-013-0387-7>
- Ozcep F, Zarif H (2006) Microzonation studies based on soil liquefaction: Yalova city (Turkey). In: First European Conference on Earthquake Engineering and Seismology, Switzerland, 348
- Perinçek D (1979) Geologic investigation of the Çelikhan-Sincik-Koçali (Adıyaman) area, TPAO Exploration Group, Report No.1395
- Porcino DD, Tomasello G (2019) Shear wave velocity-based evaluation of liquefaction resistance for calcareous sands of different origin. *Soil Dyn Earthq Eng* 122:235–247. <https://doi.org/10.1016/j.soildyn.2019.03.019>
- Şaroglu F, Emre O, Kusu I (1992) The East Anatolian fault zone of Turkey. *Ann Tectonicae*, VI 99–125:1992
- Seed HB (1976) Evaluation of soil liquefaction effects on level ground during earthquakes. Liquefaction Problems in Geotech. Eng. ASCE Annual Convention and Exposition, Philadelphia
- Seed HB, Idriss IM (1971) Simplified procedure for evaluating soil liquefaction potential. *J Soil Mech Found Div* 97(SM9):1249–1273. <https://doi.org/10.1061/JSFEAQ.0001662>
- Seed HB, Lee KL (1966) Liquefaction of saturated sands during cyclic loading. *J Soil Mech Found Div*. <https://doi.org/10.1061/JSFEAQ.0000913>
- Seed HB, Arango I, Chan CK (1975b) Evaluation of soil liquefaction potential during earthquakes. EERC, Berkeley, California, Earthquake Engineering Research Center, Report no

- Seed HB, Idriss IM, Arango I (1983) Evaluation of liquefaction potential using field performance data. *J Geotech Eng* 109(3):458–482. [https://doi.org/10.1061/\(ASCE\)0733-9410\(1983\)109:3\(458\)](https://doi.org/10.1061/(ASCE)0733-9410(1983)109:3(458))
- Seed HB, Tokimatsu K, Harder LF, Chung RM (1985) Influence of SPT procedures in soil liquefaction resistance evaluations. *J Geotech Geoenviron Eng* 111(12):1425–1446. [https://doi.org/10.1061/\(ASCE\)0733-9410\(1985\)111:12\(1425\)](https://doi.org/10.1061/(ASCE)0733-9410(1985)111:12(1425))
- Seed HB, Martin PP, Lysmer J (1975a) The generation and dissipation pore water pressures during soil liquefaction. Earthquake Engineering Research Center, Report no: EERC 75–26, Berkeley, California
- Seymen I, Aydın A (1972) Bingöl deprem fayı ve bunun Kuzey Anadolu Fayı ile ilişkisi, *M.T.A. Bull* 79:33–39 (in Turkish)
- Stokoe KH II, Roesset JM, Bierschwale JG, Aouad M (1988) Liquefaction potential of sands from shear wave velocity. In: *Proceedings 9WCEE*, 3: 213–218.
- Sunkar M, Tonbul S (2013) İluh Deresi Batman Havzası'nın Jeomorfolojisi, İstanbul Üniversitesi Edebiyat Fakültesi Coğrafya Bölümü Coğrafya Dergisi, 24, 38–60, İstanbul (in Turkish)
- Taymaz T, Eyidoğan H, Jackson J (1991) Source parameters of large earthquakes in the East Anatolian Fault Zone (Turkey). *Geophys J Int* 106(3):537–550. <https://doi.org/10.1111/j.1365-246X.1991.tb06328.x>
- Tocher D (1958) Earthquake energy and ground breakage. *BSSA* 48(2):147–153. <https://doi.org/10.1785/BSSA0480020147>
- Tokimatsu K, Yoshimi Y (1983) Empirical correlation of soil liquefaction based on SPT N-value and fine content. *Soils Found* 23(4):56–74. https://doi.org/10.3208/sandf1972.23.4_56
- Toksoz MN, Shakal AF, Michael AJ (1979) Space-time migration of earthquakes along the north Anatolian fault zone and seismic gaps. *PAGEOF* 117(1979):1258–1270. <https://doi.org/10.1007/BF00876218>
- Tuna D (1973) VI. Explanatory report of the nomenclature of regional lithostratigraphic units. TPAO Search Group, Archive No.813
- Tunusluoglu MC, Karaca O (2018) Liquefaction severity mapping based on SPT data: a case study in Canakkale city (NW Turkey). *Environ Earth Sci* 77:422. <https://doi.org/10.1007/s12665-018-7597-x>
- Ulamis K, Kilic R (2008) Liquefaction potential of Quaternary alluvium in Bolu settlement area, Turkey. *Environ Geol* 55:1029–1038. <https://doi.org/10.1007/s00254-007-1052-8>
- Ulamis K, Kilic R (2012) Liquefaction potential evaluation of the quaternary alluvium, Western Ankara (Turkey). *Environ Earth Sci* 67:945–958. <https://doi.org/10.1007/s12665-012-1526-1>
- Ulusay R, Tuncay E, Sönmez H, Gökçeoğlu C (2004) An attenuation relationship based on Turkish strong motion data and iso-acceleration map of Turkey. *Eng Geol* 74(3–4):265–291. <https://doi.org/10.1016/j.enggeo.2004.04.002>
- Ulutas E, Ozer MF (2010) Empirical attenuation relationship of peak ground acceleration for Eastern Marmara region in Turkey. *Arab J Sci Eng* 35:187–203
- Uyanık O (2002) Kayma Dalga Hızına Bağlı Potansiyel Sıvılaşma Analiz Yöntemi. Doktora Tezi DEU Fen Bilimleri Enstitüsü, İzmir (in Turkish)
- Uyanık O (2006) Sıvılaşır yada Sıvılaşmaz Zeminlerin Yinelemeli Gerilme Oranına Bir Seçenek, DEU Mühendislik Fakültesi Fen ve Mühendislik Dergisi Cilt:8, Sayı 2:79–91 (in Turkish)
- Uyanık O (2010) Compressional and shear-wave velocity measurements in unconsolidated top-soil and comparison of the results. *Int J Phys Sci* 5(7):1034–1039
- Uyanık O (2011) The porosity of saturated shallow sediments from seismic compressional and shear wave velocities. *J Appl Geophys* 73(1):16–24. <https://doi.org/10.1016/j.jappgeo.2010.11.001>
- Uyanık O (2020) Soil liquefaction analysis based on soil and earthquake parameters. *J Appl Geophys* 176:104004. <https://doi.org/10.1016/j.jappgeo.2020.104004>
- Uyanık O, Taktak AG (2009) Kayma Dalga Hızı ve Etkin Titreşim Periyodundan Sıvılaşma Çözümlemesi için Yeni Bir Yöntem. Süleyman Demirel Üniversitesi Fen Bilimleri Enstitüsü Dergisi 13(1):74–81 (in Turkish)
- Uyanık O, Ekinci B, Uyanık NA (2013) Liquefaction analysis from seismic velocities and determination of lagoon limits Kumluca/ Antalya example. *J Appl Geophys* 95:90–103. <https://doi.org/10.1016/j.jappgeo.2013.05.008>
- Wells DL, Coppersmith KJ (1994) New empirical relationships among magnitude, rupture length, rupture width, rupture area, and surface displacement. *BSSA* 84(4):974–1002. <https://doi.org/10.1785/BSSA0840040974>
- Yoshimi Y (1967) An experimental study of liquefaction of saturated sands. *Soils Found* 7(2):20–32. https://doi.org/10.3208/sandf1967.7.2_20
- Youd TL, Idriss IM, Andrus RD, Arango I, Castro G, Christian JT, Dobry R, Finn WDL, Harder LF, Hynes ME, Ishihara K, Koester JP, Liao SSC, Marcuson WF, Martin GR, Mitchell JK, Moriawaki Y, Power MS, Robertson PK, Seed RB, Stokoe KH (2001) Liquefaction resistance of soils: summary report from the 1996 NCEER and 1998 NCEER/NSF workshops on evaluation of liquefaction resistance of soils.

- J Geotech Geoenviron Eng 127(10):817–833. [https://doi.org/10.1061/\(ASCE\)1090-0241\(2003\)129:3\(284\)](https://doi.org/10.1061/(ASCE)1090-0241(2003)129:3(284))
- Zarif H, Özçep F, Özyalın Ş (2005) Soil liquefaction based microzonation: the example of Yalova. Kocaeli University, Kocaeli, Earthquake Symposium
- Zarif H, Özçep F, Seyyar T (2004) Liquefaction hazard analysis of alluvial soils in Yalova, Turkey. In: 16th International Geophysics Congress, Ankara

Publisher's Note Springer Nature remains neutral with regard to jurisdictional claims in published maps and institutional affiliations.

Springer Nature or its licensor (e.g. a society or other partner) holds exclusive rights to this article under a publishing agreement with the author(s) or other rightsholder(s); author self-archiving of the accepted manuscript version of this article is solely governed by the terms of such publishing agreement and applicable law.